Doctoral Dissertation

Development of Analytical Technique for Simultaneous Detection of Cyanide, Thiocyanate, and Selenocyanate in Living Mammalian Cells

2023

Aphinan Hongprasit

Graduate School of Pharmaceutical Sciences, Chiba University

TABLE OF CONTENTS

		Page
SUM	IMARY	iii
CHA	APTERS	
1	. Introduction	1
2	Literature review.	1
	Cyanide	1
	Thiocyanate	3
	Selenocyanate	4
	Analysis of Cyanide, Thiocyanate, and Selenocyanate	5
	Fluorescence Detection and König Reaction	8
	Inductively coupled plasma mass spectrometry (ICP-MS)	11
	Myeloperoxidase and its inhibitors	12
3	. Comparison of quantification of cyanide, thiocyanate, and	
	selenocyanate by HPLC-fluorescence detector with post-column	
	könig reaction and thiocyanate and selenocyanate by HPLC-	
	inductively coupled plasma mass spectrometer	14
	Introduction	14
	Material and Methods	15
	Results and Discussion.	18
4	. Simultaneous detection of thiocyanate and selenocyanate in living	
	mammalian cells including A549, HepG2, HEK293 and PC12	
	cells	26
	Introduction	26
	Material and Methods	26

		Page	
	Results and Discussion.	28	
5.	Effect of myeloperoxidase on intracellular thiocyanate and		
	selenocyanate generation	38	
	Introduction	38	
	Material and Methods	38	
	Results and Discussion.	40	
6.	Conclusion.	44	
	References	46	

SUMMARY

1. Comparison of Quantification of Cyanide, Thiocyanate, and Selenocyanate by HPLC-Fluorescence Detector with post-column König reaction and Thiocyanate and Selenocyanate by HPLC-inductively coupled plasma mass spectrometer.

Although it is well known that cyanide (CN) is highly toxic to living mammalian cells, it has been currently suspected to be endogenously generated in mammalian cells. Selenocyanate (SeCN) is a newly discovered selenium metabolite in various mammalian cells, and it is presumably related to amelioration of selenite toxicity by endogenous CN. Recently, it was reported that the detection of CN, SeCN and thiocyanate (SCN) was simultaneously performed by HPLC-fluorescence detector (FLD) with the post-column König reaction. Besides, SeCN and SCN are also detectable by the HPLC-inductively coupled plasma mass spectrometer (HPLC-ICP-MS) due to the detections of selenium and sulfur, respectively. ICP-MS is known that it is a highly sensitive technique for the detections of selenium and sulfur, and robustness against sample matrices. In this chapter, HPLC-FLD with the post-column König reaction and HPLC-ICP-MS were compared in terms of the sensitivity and the linearity of SCN and SeCN detection. Moreover, CN ion was also evaluated the parameters of determination using HPLC-FLD with the post-column König reaction.

As previously reported, SCN and SeCN were able to be detected by HPLC-ICP-MS and HPLC-FLD. The linearity of calibration curves was verified by calculated R^2 values of more than 0.990. The limit of detection (LOD) for SCN indicated that HPLC-FLD with the post-column König reaction showed 354 times more sensitive than HPLC-ICP-MS. Likewise, the LOD for SeCN indicated that HPLC-FLD showed 51 times more sensitive than HPLC-ICP-MS. HPLC-FLD with the post-column König reaction also provided the LOD for CN at 9.37 nM. In addition, HPLC-FLD provided the shorter elution time than HPLC-ICP-MS, which was advantageous for the analysis of target compounds.

These results indicated that HPLC-FLD was a more superior technique to detect SeCN and SCN than HPLC-ICP-MS, and the detection of CN ion was also an advantage of HPLC-FLD.

2. Simultaneous Detection of Thiocyanate and Selenocyanate in Living Mammalian Cells Including A549, HepG2, HEK293 and PC12 cells.

As shown in Chapter 1, HPLC-FLD with the post-column König reaction is the superior technique to HPLC-ICP-MS for the simultaneous detection of SCN and SeCN. In this chapter, the amounts of SCN and SeCN in various mammalian cell lines exposed to selenite were quantified by the suitable analytical technique, i.e., HPLC-FLD with the post-column König reaction, to reveal the detoxification of selenite by its biotransformation to SeCN.

Four kind of mammalian cell lines, A549, HepG2, PC12, and HEK293 were separately seeded, cultured, and then divided into two groups. One group was exposed to sodium selenite at two non-toxic concentrations for each cell type obtained from the cytotoxicity tests. The other group was treated under normal conditions serving as a control. Namely, A549, HepG2, and PC12 cells were treated with 2.5 and 5 μM sodium selenite, and HEK293 cells were treated with 1 and 2.5 μM sodium selenite for 24 h before being collected with a 250-μL aliquot of cold 0.5x PBS to perform the micro liquid extraction. The cell suspension was homogenized, and then proteins were removed by adding a 200-μL aliquot of ice-cold acetone. The sample mixture was centrifuged to obtain the supernatant, and then stabilized by adding bicarbonate buffer. The solution was filtered, and the filtrate was subjected to the HPLC-FLD.

HPLC-FLD with the post-column technique gave us good separation of SCN and SeCN spiked in HepG2 supernatant by the pretreatment of ice-cold acetone as a deprotein agent. However, the detection of intracellular CN cannot be accomplished by this technique due to enormous matrix peaks overlapping with the retention time corresponding to CN ion. To more clearly and specifically detect CN, the pretreatment conditions should be more carefully evaluated in future studies. The total amounts of intracellular SCN and SeCN in selenite-exposed A549, HepG2, and PC12 cells were significantly increased but no increase was observed in HEK293 between the selenite-exposed and control groups. These results indicate that the selenite-tolerant cell lines such as A549, HepG2, and PC12 can induce endogenous CN to form SCN and SeCN. Since SeCN was more produced than SCN at the higher concentration, selenium and sulfur seemed to be competitively transformed to SeCN and SCN, respectively, with endogenous CN. In this chapter, I conclude that endogenous CN is one of detoxification factors for selenite toxicity.

3. Effect of Myeloperoxidase on Intracellular Thiocyanate and Selenocyanate Generation.

In the second chapter, I proposed that endogenous CN seemed to play an important role in the detoxification of selenium although CN was recognized as a highly toxic substance. In this chapter, I intended to reveal how endogenous CN was produced in mammalian cells. Myeloperoxidase (MPO), a heme protein expressed in phagocytic cells, generates reactive oxygen species accelerating tissue damages during inflammation. Some preceding studies suggested that MPO is one of key enzyme to produce endogenous CN. Namely, it is well known that hypochlorous acid (HOCl), a robust cytotoxic oxidant, can be produced by MPO. HOCl can oxidize glycine resulting in the production of cyanogen chloride (CNCl) through the chlorination reaction under acidic conditions. On the other hand, MPO is known to be specifically expressed in neutrophils. A human leukemia cell line, HL60, is known to express MPO. Indeed, previous studies indicated that the generation of endogenous CN was accelerated in HL60 under oxidative stress. This evoked us that HL60 may more efficiently produce SCN and SeCN derived from endogenous CN than another leukemia cell line, K562, which was lacking the expression of MPO. In addition to the leukemia cell lines, human hepatoma cell line, HepG2 was also evaluated because endogenous CN was ubiquitously observed in mammalian cells. To clarify the role of MPO to produce endogenous CN, an MPO inhibitor, AZD3241, was used to evaluate the intracellular biotransformation of SCN and SeCN.

HL60, K562, and HepG2 cells were pretreated with AZD3241 for 24 hrs, and then three cell lines were exposed to sodium selenite at the highest non-toxic concentration levels for additional 24 hrs. The cells were collected to perform HPLC-FLD for the determination of intracellular SCN and SeCN. The results indicated that the MPO inhibitor, AZD3241, significantly decreased the amounts of intracellular SCN and SeCN in all cell lines, i.e., HL60, K562, and HepG2 cells. The inhibition in HL60 was easily explainable because HL60 was expressing MPO. However, the inhibitory effect of AZD3241 was also observed in K562 and HepG2. This suggested that endogenous CN could be generated by an MPO-like enzyme that was inhibited with AZD3241. This putative enzyme with an MPO activity should be identified in future sequencing studies to clarify the inconclusive mechanism of endogenous CN generation.

In conclusion, these data provide insights the detection of SCN and SeCN obtained by HPLC-FLD with post-column König reaction was more 354 times and 51 times sensitive than by HPLC-ICP-MS, respectively. I found that HPLC-FLD with post-column König reaction was a superior technique for detecting and quantifying SCN and SeCN to HPLC-ICP-MS. It was applicable to separate and detect intracellular SCN and SeCN in

mammalian cell lines exposed to selenite. In addition, MPO can affect the production of intracellular SCN and SeCN through the test with MPO-inhibitor, and some MPO-like enzymes may also involve in this mechanism, which need to be identified in future sequencing experiments.

CHAPTER 1

Introduction

Cyanide (CN) is one of the most critical toxic substances. In addition, it is also generated endogenously. There are many studies and research on the toxic mechanism and the effects of CN at present. However, studies on endogenous CN, in particular, how it is generated, and its role in cellular function, are still critical issues and questions. Recent studies on selenium toxicity have revealed a new intracellular metabolite of selenium, selenocyanate. This metabolite is established by forming selenium and CN even though no additional exogenous CN was used in this experiment, evoking us that endogenous CN has a trippy effect on human health. For instance, it plays an essential role in attenuating the toxic effects of other toxic substances in cells. However, precise determination of the endogenous CN content remains challenging because of its short half-life and instability under a typical ambient condition. Pretreatments of a CN analysis are also necessary as well as the CN analysis. Moreover, the simultaneous analysis of significant metabolites of CN, such as thiocyanate (SCN) and selenocyanate (SeCN), is another important issue.

This study's first aim is to compare and develop the best analytical method for simultaneously detecting CN, SCN, and SeCN in mammalian cells. They will be compared in terms of sensitivity and linearity for analysis. The mammalian cell lines were incubated with selenite to determine the metabolites and the affinity established in the cells. The production of selenium and CN-related metabolites in cells was further tested with MPO enzyme inhibitors, which have been studied as the enzymes that play an essential role in human CN production. In this test, alteration in CN analog metabolites is observed.

Through this experiment and research, I hope to gain more knowledge and analytical and experimental skills about CN and selenium. These findings will help answer a variety of questions and will provide additional questions and issues for further research into CN toxicology in the future.

CHAPTER 2

Literature Review

Cyanide

Cyanide (CN) is a potentially toxic substance that rapidly inhibits respiration, i.e., mitochondrial oxidative phosphorylation (1). It can also affect critical cellular ion

homeostasis (2). A simple mechanism of cytotoxicity of CN can occur via the binding of mitochondrial electron transport Complex IV (cytochrome C oxidase). It leads to rapid inhibition of aerobic adenosine triphosphate (ATP) generation irreversibly and consequent cell dysfunction or death (3,4). CN can bind to oxidized and reduced forms of cytochrome C oxidase, but it has a higher specificity with the oxidized form (5). CN can be converted enzymatically to SCN by rhodanese in the liver (Figure 2.1). It is then excreted normally through the kidneys with its high solubility and is less biologically and toxicologically inert than CN..

The constituent properties of CN (i.e., KCN, NaCN, CuCN, AgCN, and HCN) are one of the main factors that substantially affect their bioavailability and are associated with CN poisoning in the human body. CN can produce fatal toxicity rapidly resulting from its rapid absorption and ability to diffuse into the bloodstream and tissues, leading to its binding to metalloenzymes and inhibiting enzyme activity (6). Thus, tissues and organs are severely affected because CN can be absorbed and distributed very quickly (7–9). HCN is a form of CN existing in a gaseous state and is readily soluble in water and biological fluids. Over 98% of CN exists as a volatile soluble form (HCN) at the pH of biological fluid because of its weakly acidic properties (pKa = 9.2). CN could be the potential substance for mediating biological functions because it has some advantages in its molecule size and water solubility (10,11). Several forms of CN are known in the environment, for example, gaseous hydrogen CN (HCN), water-soluble CN salts with potassium (K) and sodium (Na), poorly water-soluble CN salts with copper (Cu), gold (Au), mercury (Hg), and silver (Ag). As biological CN compounds, vitamin B₁₂ and cyanogenic glycosides are known (12). Cyanogenic glycosides and nitrile-containing compounds that release free CN are known as cyanogens (13,14). Amygdalin is one of the most famous cyanogenic compounds and is found in some plants, especially in apricot pits, apple seeds, or almond husks (15). It is known that almost exogenous CN in the human body originates from tobacco which is measured in the form of HCN at more than 200 mg per cigarette (16). Other sources of CN exposure include exposure to industrial processes and their byproducts.

On the other hand, some works of literature report that CN is also metabolically generated by the chlorination of glycine catalyzed by human myeloperoxidase (MPO) during body injury or inflammation (17). The biological production of CN is also known as bacterial cyanogenesis by *Pseudomonas aeruginosa* (during the infection on wounds

and lungs of immune-compromised patients as an opportunistic pathogen) (18,19). These biologically generated CN is recognized as endogenous CN.

The detection of endogenous CN has previously been demonstrated in some mammalian cells, where different methods can measure it, and the baseline level of CN was found at low nanomolar to micromolar concentrations (11). However, the detection of CN in cell and tissue samples is not accessible due to the complex matrices.

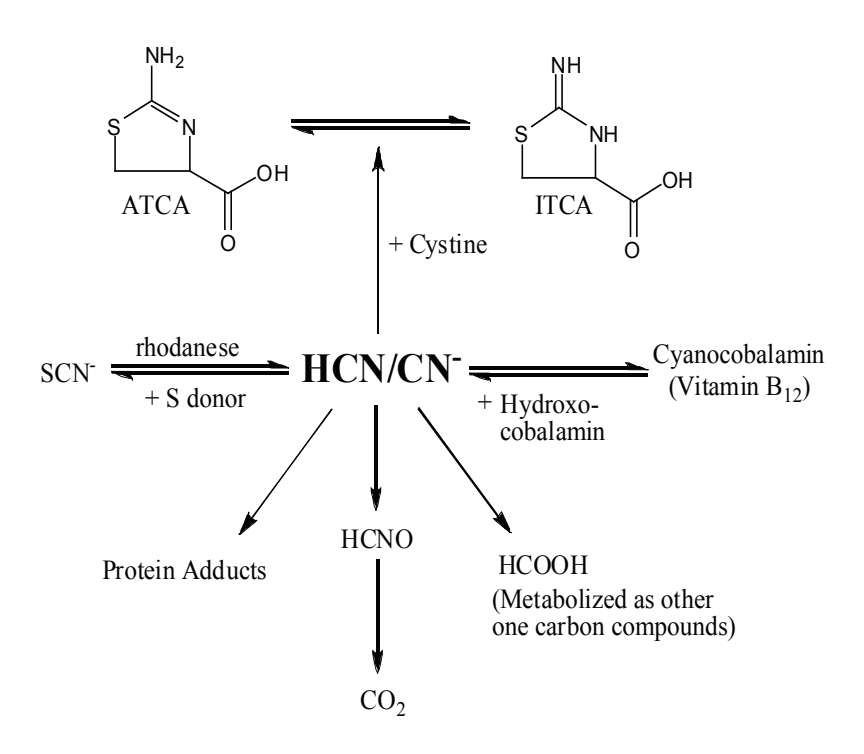


Figure 2.1. Metabolism of cyanide in human body. Sources: Logue BA, Hinkens DM. The Analysis of Cyanide and its Metabolites in Biological Samples. In 2008.

Thiocyanate

Thiocyanate (SCN⁻, hereinafter SCN) is the primary metabolite of CN (20). This fact is well known because of the major pathway detoxification of CN by rhodanese or 3-mercaptopyruvate sulfurtransferase (MST) with thiosulfate (S₂O₃²⁻) (21–23). The transfer of a sulfane sulfur atom from sulfur donors can be catalyzed by these enzymes, as mentioned above, and sulfane sulfur reacts with CN irreversibly. SCN is readily excreted into the urine. Rhodanase and MST enzymes are abundant in the liver and kidneys, located on the membrane of mitochondria (24,25). SCN is usually contained in biological fluids such as serum, saliva, and urine (12). The negligible concentration of nutritional SCN originates in SCN-containing foods such as dairy products (26) where SCN in blood plasma

is actively transported (27). Various papers demonstrated that SCN concentration in human biological fluid is relatively elevated by CN exposure through inhalation of CN by cigarette smoking (28), ingestion of CN in cases of suicide (29), and clinical use of sodium nitroprusside (30). It is clearly demonstrated that there are differences in the concentration between non-smokers and smokers. The saliva SCN concentrations of non-smokers are 0.5–2 mM, while smokers have the average SCN concentration in smokers around 3 mM, and SCN concentrations may rise to 6 mM in some smokers (31–33). Some epidemiological studies showed that the vegetarian diet also affects SCN levels, and vegetarians have high SCN levels in the body (34). It was twice as high in the regular diet group. In addition, biological SCN is also generated from cyanogenesis by *Pseudomonas aeruginosa*, mainly found in the lungs of immunocompromised patients and infected wounds (35).

Several studies have clearly shown that SCN is the main metabolite of CN by the detoxification of CN, and approximately 80% of CN are metabolized by this pathway (36,37). In contrast, the remaining around 15% are transformed by other pathways, such as reacting with cysteine to form 2-amino-2-thiazoline-4-carboxylic acid (ATCA) and its tautomer 2-iminothiazolidine-4-carboxylic acid (ITCA) (38,39). Therefore, SCN may be a useful indicator of the presence or exposure of CN in the body.

Selenocyanate

Selenocyanate (SeCN-, from now on, SeCN) is a newly discovered metabolite of selenium (Se) in mammalian cells (40). SeCN is a chemical analog of SCN. As mentioned above, SCN is endogenously produced by the reaction between CN and thiosulfate (S₂O₃) with rhodanese in the liver to detoxify CN toxicity. On the other hand, it is suggested that SeCN is generated in mammalian cells by a non-enzymatic reaction between selenide (Se²⁻) and endogenous CN when the cells are exposed to excessive amounts of selenite (SeO₃²⁻) (40). That is, it does not require rhodanese, and the critical reaction relies on the high reactivity of selenium. In addition, the replacement of selenosulfate (SeSO₃²⁻) with SeO32-more efficiently produces SeCN. According to the enzymatic mechanism of rhodanese, it is explainable that the production of CySSH persulfide is the intermediate at the reaction of Cys-247 with S₂O₃²⁻, then a reaction with CN occurs to regenerate Cys-247 resulting in the production of SCN (41,42). It is assumed that chemical species such as GSSeH may interact with CN *in vivo* to produce SeCN due to the higher reactivity of Se (43).

The cytotoxicity of SeCN is apparently lower than SeO₃²⁻ and CN. It is profoundly relevant to ameliorating SeO₃²⁻ toxicity by endogenous CN (40). It is also reported that radioisotope-labeled carbon in SeCN was metabolized to SCN to utilize Se as an essential element *in vivo* when SeCN is used as a nutritional source of Se in rats (44). These findings indicate a circulating relevance between SCN and SeCN in living organisms. The analytical techniques targeting SCN and SeCN with high selectivity and sensitivity are necessary to elucidate the biotransformation between SCN and SeCN. The techniques should be robust against a complex matrix to be applicable to living cells.

Analysis of Cyanide, Thiocyanate, and Selenocyanate

The development of the method for CN analysis on biological samples is essential for many reasons, including the determination of CN exposure in humans, experimental studies on the toxicity of CN, CN intoxication or therapeutic use, and the CN concentrations monitoring for cyanogenic-receiving individuals (36,45). Humans may be exposed to CN from many exogenous sources, for example, dietary, environmental, industrial, inhalation of tobacco smoke, and other sources. In addition, there are many sources of endogenous CN, such as the chlorination of glycine by human MPO (17), the conversion of other CN derivatives, metabolism of vitamin B12 (46), or even bacterial cyanogenesis by Pseudomonas auruginosa (18)(19). CN is rapidly distributed in the body through the bloodstream after ingestion. Although a variety of analytical techniques are available, many complicated factors for CN analysis, such as the short half-life of CN in vivo (36,45,47), the instability of CN contents under typical storage conditions, and even significant endogenous concentrations of CN in biological matrices (48-50) make CN detection extremely challenging. It is well known that CN in the human body is rapidly biotransformed to the significant metabolite as SCN. Some reports have directly determined SCN in biological fluids as a measurement of CN as described whether the plasma concentration of SCN has also been used as an index of long-term exposure to cigarette smoke (51).

The problematic nature of CN analysis in biological samples, the most appropriate biological sampling technique, storage conditions, sample preparation, and analysis techniques must be dissolved with cautions by selecting the most precisely accurate analytical method to ensure the accurate CN determination.

Spectroscopic methods

The canonical methods for measuring CN and their derivatives are spectrophotometry and fluorometry. These methods have been used as the primary analytical technique for evaluating CN-containing samples. Many of the earliest spectroscopic methods studies relied on König reactions to produce spectrophotometrically active products (52–54). For instance, Morgan and Way (1980) used the König reaction for the spectroscopic analysis of CN concentrations in blood. CN determination was performed through the separation in a microdiffusion cell. CN-trapped alkaline solution with sodium *N*-chloro-p-toluenesulfonamide (chloramine T-phosphate) to generate the conversion of CN to cyanogen chloride (CNCl) and pyridine-pyrazolone reagent reacted to the intermediate ion. The resulting solution was analyzed fluorometrically (55). They detected CN in the solution by the fluorescent quinone derivatives. This method was also applied for biological fluids by reacting *p*-benzoquinone with CN in DMSO to generate green fluorescence.

In addition, simultaneous detection of CN and SCN was conducted spectrophotometrically. Pettigrew and Fell (1972) detected CN and SCN in human plasma samples using trichloroacetic acid deproteinization. Then, the bromination reaction of supernatant with the treatment of pyridine-phenylene diamine was conducted. Good recovery and high sensitivity of detection were obtained (56). McMillan and Svoboda (1982) also determined that CN and SCN are contained in human red blood cell suspension with good recovery (57). There is a report determining CN and SCN simultaneously by fluorometric detection with König reaction. Toida *et al.* (1984) performed their study on blood plasma and red blood cell suspension that provided good linearity, sensitivity, and precision for their samples. This study also applied to the quantification of CN and SCN in the blood of smokers and non-smokers (28).

Overall, spectroscopic analysis methods often use relatively simple and inexpensive equipment, which has made them so popular and widely used. However, this method relies on complex reactions to analyze CN and their derivatives from biological matrices. In addition, most techniques for CN analysis require microdiffusion or other time-consuming sample preparation techniques to achieve accurate measurement, good recoveries, and sufficient detection limit.

Gas Chromatography

Gas chromatography (GC) is another popular analytical technique for CN and SCN because of the low detection limit, and the easier sample preparation of CN determination

has been achieved (58,59). With this analytical technique, headspace (HS) sample preparation is typically performed prior to GC analysis. HS and microdiffusion in the CN extraction are similar principles that HCN released by adding a strong acid to perform the conversion of CN will be collected in the headspace of a sealed vial. Free HCN can be analyzed by various detectors (50,60–62). Standard detectors for CN analysis are the nitrogen-specific detector (NPD) (63,64), the electron capture detector (ECD) (60,62), or the mass spectrometry (MS) detector (58,65,66). NPD is widely used for CN analysis due to its good selectivity and sensitivity for the analyte by detecting nitrogen and phosphorus-containing compounds. ECD is beneficial for analysis as it has good sensitivity and stability, which are advantages over NPD. The advantages of the MS detector include excellent selectivity, sensitivity, identification of the analyte, and the ability to distinguish between CN isotopes, which can significantly improve the accuracy and precision of CN analysis.

When the simultaneous determination of CN and SCN is needed, HS analysis cannot be used because SCN cannot provide enough vaporization. Therefore, derivatization with pentafluorobenzyl bromide (PFB-Br) with subsequent GC analysis has been performed for the simultaneous analysis of these two targeted substances (67–69). Analytical methods for the detection and quantification of CN by GC have been developed and reported extensively as they are helpful for the analysis of CN due to HCN fluctuations. The major disadvantage of using GC for HCN analysis is its low molecular weight. It may cause difficulty in the chromatographic separation of HCN from other small molecular weight compounds of the sample. Furthermore, some analytes with shallow evaporation pressures, e.g., SCN, require derivatization through complex reactions before they can be analyzed. Therefore, although GC analysis of CN offers many advantages, highly efficient liquid chromatography methods have also been developed as alternative chromatography methods for CN analysis.

High-performance liquid chromatography

High-performance liquid chromatography (HPLC) is required to detect CN, SCN, and SeCN to derivatize an ultimate detectable compound except for ion chromatography. The standard HPLC systems to detect CN, SCN and SeCN rely on two different chemical reactions that yield chemical complexes. One is the NDA-taurine interaction, and the other is König reaction which is more widely used. These reactions are precise to form a fluorescent substance, which can only be accomplished in the presence of a CN molecule or a CN group in its molecule.

Several studies used the NDA reaction to detect CN, SCN, and SeCN in biological samples by HPLC with good sensitivity and reliability. Human urine was applied this analytical method by Sano *et al.* (1989) (70), and then they also applied this method to the measurement of CN in human blood (71). HPLC-MS/MS with the NDA reaction was improved by Mottier *et al.* (2010) (72) to analyze HCN in a cigarette smoker. Simultaneous determination of CN and SCN with NDA was also utilized by Bhandari *et al.* (2014) to produce the method with low LOD and an excellent linear range for CN analysis (73).

HPLC with the König reaction has also been developed to analyze CN, SCN, and SeCN. The König reaction has also been used for the HPLC analysis of CN. For instance, Toida *et al.* (1984) developed a technique for analyzing CN and SCN in blood plasma and red blood cells. The LOD was 0.52 μg/L with an excellent linear range of 1.3–260 μg/L by this analytical method (28). This technique, HPLC with fluorometric detection of the König reaction, made the simultaneous detection of CN and SCN possible. HPLC with the König reaction using a post-column was recently applied to SeCN in whole blood and cultured mammalian cells by Mochizuki *et al.* (2019) (74). It was the first simultaneous detection of SCN and SeCN in biological samples with LOD at 7.35 nM of LOD and an excellent linear range of 0–10 mM.

Ion chromatography (IC) is another liquid chromatographic technique for analyzing CN in biological fluids despite high LOD and time-consuming analysis. The IC method for the analysis of CN in blood was developed by Chinaka *et al.* (1998) (75). Before the IC separation, the extraction of CN was performed with methanol and water, and then, the extract was subjected to the NDA-taurine reaction for fluorometric detection.

As mentioned above, the HPLC methods for detecting CN, SCN, and SeCN in biological samples have been successfully developed. The advantages of this analytical method provide very consistent separation, excellent LOD, and good reproducibility. However, this technique has some drawbacks that cannot directly analyze CN, SCN, and SeCN. Therefore, other complex chemical reactions are required to produce a fluorescent substance due to the separation and the detection of the analytes by chromatographic method (76,77).

Fluorescence detection and König Reaction

Fluorescence detection has several advantages in specificity and sensitivity. Since fluorescent compounds emit their specific wavelength, interference from sample matrices is avoidable. The specific fluorescent emission is also helpful for the identification of the compound. Second, this assay is highly sensitive, i.e., generally 1,000 - 500,000 times better than the absorbance measurements. Third, the analytical method is simple, fast, and inexpensive. Therefore, this technique is widely applied in medicine, industry, environmental sciences, and biology.

The principle of fluorometric measurement can be explainable; the electrons are typically in pairs in the ground state (S). When it is energized by short-wavelength light, the single electron gains a higher energy and moves up to a higher orbital. According to the level of received energy (S₀, S₁, S₂,.....) (Figure 2.2), when the electron returns to the ground state, it emits fluorescence with a wavelength equal to the absorbed wavelength known the resonance fluorescence. However, in the reentry of the electrons of the emitting atoms, part of their energy is lost due to collisions and vibrations of atoms and the transfer of energy to the solution. These factors cause the light emitted when returning to the ground state to have a longer wavelength than the absorbed light, known as direct line fluorescence. This emission type is "fluorescence" with $10^{-7} - 10^{-9}$ seconds. Some emitting substances with high-energy electrons (S) are converted to electrons. High energy with similar levels is called a triplet state (T) (Figure 2.2).

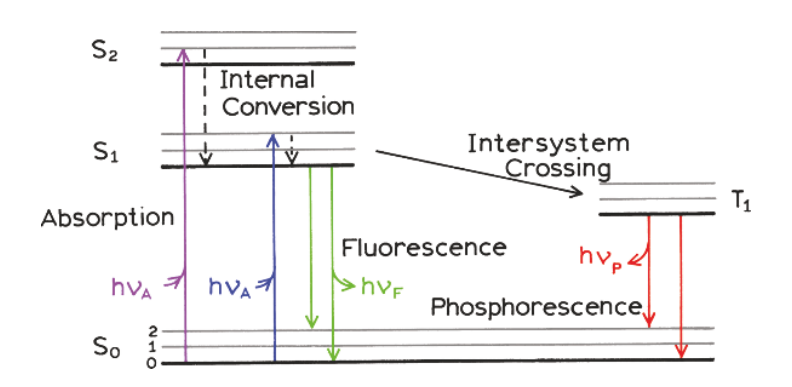


Figure 2.2. A typical Jablonski diagram illustrates the absorption, emission spectra and vibrational energy levels.

Source: Lakowicz JR, editor. Introduction to Fluorescence BT - Principles of Fluorescence Spectroscopy. In Boston, MA: Springer US; 2006. p. 1–26.

Typically, some energy loss is followed by the return of the electron to its ground state with the emission of longer wavelength light. Nevertheless, the transition of an electron from the triplet state to the ground state takes more than 10^{-7} seconds to several seconds. It is possible to see the light emitted for a long time even after the incident light has stopped at a particular wavelength known as phosphorescence (78).

The König reaction is specific and quantitative. It has been used to measure CN and relative substances by oxidation CN⁻ to a cyanogen halide, CNCl (Figure 2.3), in which CN⁺ acts as the reactive species. The CN⁺ reacts with pyridine to produce an intermediate that hydrolyzes to a conjugated dialdehyde, glutaconaldehyde. Glutaconaldehyde is coupled with a primary amine or a compound containing reactive methylene hydrogens (RH₂), such as barbituric acid, which contains a primary amine on its molecule. The reaction of this aldehyde with two molecules of 1,3-dimethyl barbituric acid generates a fluorescent dye that can be detected spectrophotometrically (79,80). This reaction can only be completed in the presence of a CN molecule or a CN derivative such as SCN or SeCN (28,74).

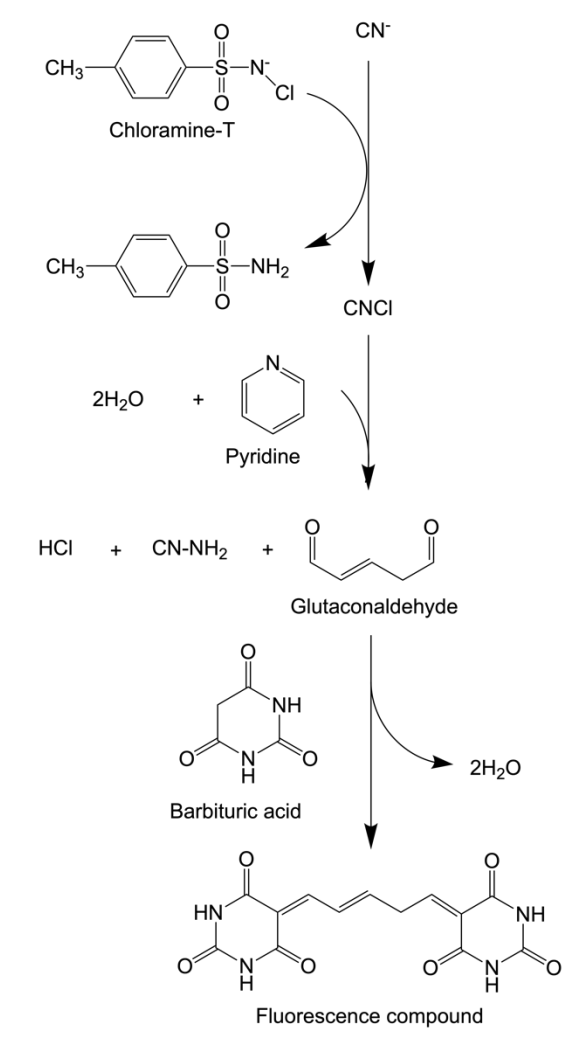


Figure 2.3. König reaction in which cyanogen chloride (CNCl) is synthesized by reaction of CN- and chloramine-T. CNCl is then converted to glutaconaldehyde by reaction with pyridine and finally converted to a fluorescence compound by reaction with barbituric acid.

Inductively coupled plasma mass spectrometry (ICP-MS)

Inductively coupled plasma mass spectrometry (ICP-MS) is an elemental analytical technique. It has some advantages, such as multi-elemental analysis at parts per trillion

(ppt) or parts per quadrillion (ppq) level. It applies to various samples such as soil, water, plants, animal tissue, and culture cells. The process of ICP-MS analysis uses plasma energy to shoot electrons from the outer ring of an atom. This results in the formation of positively charged ions of the sample to be measured. These ions are separated and measured by the mass-to-charge ratio. The signal intensity is directly correlated with the sample concentration. The analytical method can be described briefly in (**Figure 2.4**). The sample solution is atomized into an aerosol through a nebulization process, and the aerosol is transported to the argon plasma in the ICP torch (**Figure 2.5**). The elements are ionized in the ICP. Uncharged elements are removed in the particle beam at the ion lens, allowing only ions to pass into the mass spectrometer. The ions are separated following the mass-to-charge ratio (m/z) by a quadrupole before quantifying with an electron multiplier detector (81,82).

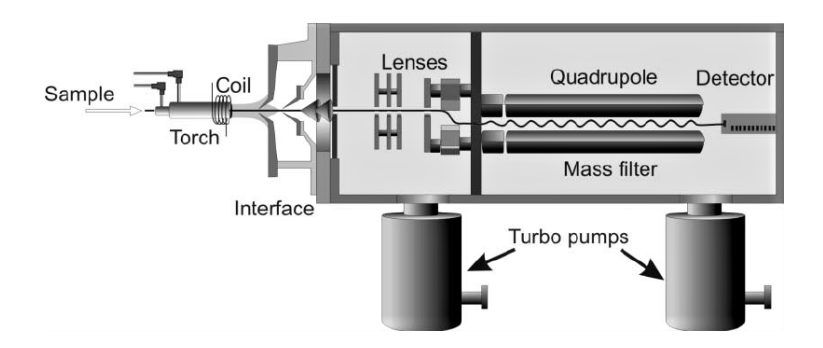


Figure 2.4. Cross-sectional schematic diagram of an ICP-MS.

Source: Wilschefski SC, Baxter MR. Inductively Coupled Plasma Mass Spectrometry: Introduction to Analytical Aspects. Clin Biochem Rev. 2019 Aug;40(3):115–33.

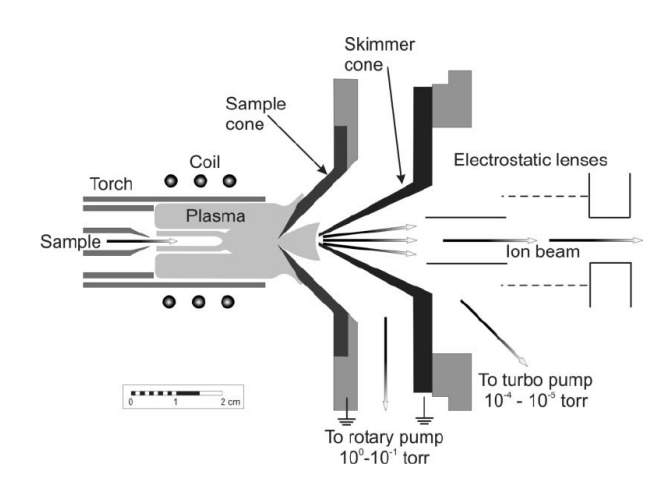


Figure 2.5. Cross-sectional schematic diagram of the interface region.

Source: Wilschefski SC, Baxter MR. Inductively Coupled Plasma Mass Spectrometry: Introduction to Analytical Aspects. Clin Biochem Rev. 2019 Aug;40(3):115–33.

Myeloperoxidase and its inhibitors

Myeloperoxidase (MPO) is abundant in neutrophils, which are the most abundant (50-70%) in all types of a white blood cells. White blood cells protect the body by decomposing xenobiotics and pathogens through phagocytosis. Within neutrophils, there are many granules, such as tertiary granules, specific granules, and azurophilic granules, called polymorphonuclear (PMN) cells (83,84). MPO is a kind of peroxidase (POD, EC 1.11.1.7) that involves the addition or the removal of hydrogen atoms or halide ions, such as halogenation. MPO is maturated by the post-translational modification to appear its specific functions (85). The structure of MPO is a di-heme protein and heterodimer. The polypeptide chains of the two units are joined together by disulfide bonds. The central region of the molecule contains iron/porphyrin-containing heme (84). The molecular weight of MPO is 144 kDa, and iron/porphyrin-containing heme consists of the active center where a specific substrate enters this site, and the substrate is catalyzed. It is reported that MPO enzymes can be found in patients with inflammatory diseases such as vasculitis, Alzheimer's disease, multiple sclerosis, lung and renal tissue injuries, and cardiovascular disease. MPO plays an essential role in bacterial infection to protect host cells from pathogen invasion because MPO can induce oxidative stress. The mechanisms for the induction of oxidative stress are explainable in that MPO catalyzes a halogenation reaction with H₂O₂ and halide as substrate and are known as the MPO- H₂O₂-halide system (86,87). In the halogenation reaction, H2O2 is the primary substrate, and another substrate is a halide ion, such as a chloride ion. MPO produces hypochlorous acid (HOCl) from chloride ions in the cell, and HOCl effectively removes bacteria and xenobiotics (87). Since MPO induces oxidative stress to eliminate bacteria and xenobiotics, it can cause injury and damage to a host's tissues and cells. The MPO-induced injury was reported in the gastrointestinal tract, oral, blood vessels, or brain (88–91).

MPO has also been found to be one of the factors involved as the possible enzyme to produce endogenous CN through *the N*-chlorination of glycine. Glycine converses into *N*-monochloroglycerine, and then, *N*,*N*-dichloroglycine and glycine are formed under acidic conditions by the dismutation. *N*,*N*-Dichloroglycine is unstable. Thus, it is readily converted into 2-cyanoacetic acid, which is further degraded into CN ion (17). Indeed, it was reported that CN was generated in leukocytes and rat pheochromocytoma cells. In particular, the CN content was increased when the MPO substrates, i.e., H₂O₂ and glycine, were exposed (92).

Two possible mechanisms for MPO inhibition are suggested. The first mechanism is related to heme-related inhibition. Namely, an iron atom in heme is targeted to irreversible MPO inhibitors by preventing H₂O₂ from accessing the active center (**Figure 2.6**). The second mechanism is the competition between an inhibitor and the MPO substrates at the active center. The inhibitor is a reversible inhibitor that forms a complex with MPO and can prevent the progression of the MPO peroxidase cycle. In other words, it serves as a precursor for MPO, resulting in a temporary cessation of the cycle by forming and accumulating compound II described in **Figure 2.6** (93).

This study used AZD3241 (Verdipersat), an irreversible MPO inhibitor and a thioxanthine analog, considering the mechanism of MPO inhibitors. It has been evaluated in various studies and is shown as an effective inhibitor of MPO in neurological and gastrointestinal diseases (94). AZD3241 was used to evaluate the effect on intracellular production of SCN and SeCN as the ultimate stable metabolites of CN.

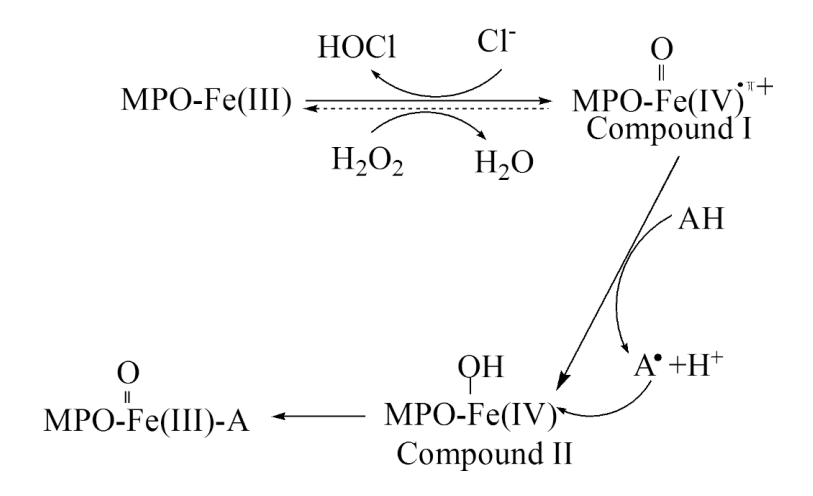


Figure 2.6. Mechanisam of irreversivle MPO inhibition by thioxanthines analogue. Radical species provided by the oxidation of thioxanthines by Compound I react with heme group of the enzyme forming covalent bond.

Source: Galijasevic S. The development of myeloperoxidase inhibitors. Bioorg Med Chem Lett. 2019;29(1):1–7.

Aims of this study

It is currently known that CN, SCN, and SeCN in mammalian cells are closely related biologically. Although cyanide is toxic to animal cells, cyanide also plays a role in attenuating selenium toxicity. CN is also transformed into less toxic compounds such as SCN and SeCN. Therefore, selecting appropriate available measurements that simultaneously determine the quantitative changes of CN, SCN, and SeCN is highly necessary. The first aim of this study was to compare and develop the best analytical

methods for the simultaneous detection of CN, SCN, and SeCN in mammalian cells. They were compared in terms of sensitivity and linearity for analysis. The second aim of this study was to develop a sample preparation method in which mammalian cells were pretreated, and their target metabolites, SCN and SeCN, were extracted and separated for chromatography. A quantitative analysis was performed on samples of mammalian cells incubated with selenite to determine the metabolites and associations established in the cells. In addition, the final aim after selecting suitable analytical and sample preparation methods for studies in mammalian cells. The production of selenium and its related metabolites in cells were further tested with MPO inhibitors, which have been studied as critical enzymes in human CN production. In this assay, changes in the analogous metabolites of CN were observed.

CHAPTER 3

Comparison of Quantification of Cyanide, Thiocyanate, and Selenocyanate by HPLC-Fluorescence Detector with post-column König reaction and Thiocyanate and Selenocyanate by HPLC-inductively coupled plasma mass spectrometer

Introduction

It is well known in the field of toxicology that CN is toxic to humans and animals due to its inhibition of oxygen consumption at the cellular level (1). Humans can obtain cyanide (CN) from various sources such as inhalation of CN, cigarette smoking, CN ingestion suicide, and sodium nitroprusside clinical treatment, which resulted in a subsequent increase in the SCN concentration in the biological fluid. Due to the rapid elimination of CN toxicity in humans by rhodonase and thiosulfate (S₂O₃²⁻) in the liver and kidneys (21,22), SCN is excreted as the primary metabolite, which has excellent water solubility. In general, small concentrations of SCN are found in human biological fluids such as serum, saliva, and urine (12), suggesting that low concentrations of SCNs in body fluids originate from the consumption of SCN-containing foods such as products as dairy products or vegetables (26,34). Therefore, the level of SCNs in biological fluids is considered a helpful indicator describing the relevance of CNs in the human body.

SeCN is a newly discovered metabolite of selenium (Se) (40). SeCN is formed in mammalian cells through an enzyme-independent interaction between selenide (Se²⁻) and

endogenous CN. SeCN is intracellularly generated when cells are exposed to excessive amounts of selenite (SeO₃²⁻). The attenuation of the cytotoxicity of SeO₃²⁻ is closely related to endogenous CN because the cytotoxic effect of SeCN is lower than that of SeO₃²⁻ and CN. It was found that SeCN could also be utilized as a source of Se *in vivo*, as radioisotopelabeled carbon in SeCN molecules has been reported to be metabolized *in vivo* (44). The *in vivo* employment of SeCN rendered the dissociation of selenium and the free CN, with the CN containing the radioisotope-labeled carbon being coupled with SeO₃²⁻ to form an SCN molecule, which ultimately has been excreted in the urine. This finding indicates that between SCN and SeCN, the biological circulation of both substances occurs in living organisms. The biotransformation between SCN and SeCN requires analytical techniques targeting SCN and SeCN with reasonable specificity and high analytical sensitivity to elucidate the utilization of targeted metabolites. The analytical technique should be robust for potentially interfering with complex matrices for use with live mammalian cells.

Several techniques for detecting SCN in various samples have been developed and published. These widely used techniques include spectrophotometric measurements (28,94–100), gas chromatography-mass spectrometry (GC-MS) (101) and inductively coupled plasma mass spectrometry (ICP-MS) (102). SeCN can be determined by electrochemical ionization mass spectrometry (ESI-MS), GC-MS and ICP-MS. Recently, the preliminary simultaneous detection of CN, SCN, and SeCN was achieved by HPLC-fluorescence detectors (FLD) with a post-column König reaction using pyridine-barbituric acid to provide the ultimate emitting compound that can be measured fluorometrically (74). SCN and SeCN can also be detected with HPLC-ICP-MS due to the detection of sulfur and selenium atoms, respectively, as ICP-MS shows high sensitivity for sulfur and Se detection and is resistant to the sample matrices (82). Therefore, The sensitivity and linearity comparison for SCN and SeCN detection between HPLC-FLD with the post-column with König reaction and HPLC-ICP-MS were conducted in this study.

Materials and Methods

Reagents

Sodium thiocyanate, sodium hydroxide, chloramine T, pyridine, and hydrochloric acid were purchased from Nacalai Tesque (Kyoto, Japan). Sodium acetate trihydrate, acetic acid (HPLC grade), and methanol (HPLC grade) were provided by FUJIFILM Wako Pure Chemical Corporation (Osaka, Japan). Potassium selenocyanate, sodium perchlorate, and ammonium acetate were provided by Merck (Darmstadt, Germany). Barbituric acid was

purchased from Tokyo Chemical Industry (Tokyo, Japan). Phosphate buffered saline (PBS) was purchased from Sigma (St. Louis, MO, USA).

Standard Solutions

Standard stock solutions at a concentration of 10 mM of each analytical targeted chemical substance, including CN, SCN, and SeCN, were prepared by dissolving each reagent in Milli-Q water (18.3 M Ω ·cm). Subsequently, the stock solutions were diluted with Milli-Q water to accomplish seven different concentrations of CN, SCN, and SeCN standard solution mixtures. The evaluation of limit of detection (LOD) and the limit of quantification (LOQ) were carried out by using CN, SCN, and SeCN standard solution mixtures at concentrations of 0.010, 0.050, 0.25, 1.0, 5.0, 7.5, and 10 μ M for HPLC-FLD. Meanwhile, only metal-containing substance, SCN, and SeCN standard solution mixtures at concentrations of 1.0, 5.0, 10, 25, 50, 75, and 100 μ M for HPLC-ICP-MS.

Apparatus and chromatographic conditions for HPLC-FLD and HPLC-ICP-MS

The HPLC-FLD for detecting and quantifying CN, SCN, and SeCN was performed according to a previously described procedure (74) with slight modification as shown schematically in **Figure 3.1**. Experiments were carried out using the HPLC system (Shimadzu LD-20 Series Prominence, Shimadzu, Kyoto, Japan) composed of a degassing unit (Shimadzu DGU-20A3R), a pump for delivering the mobile phase (LC-20LD), and a manual injector. LC-20AD and LC-20AB pumps were used to deliver the chloramine-T solution as the 1st post-column reagent and pyridine-barbituric acid solution as the 2nd post-column reagent, respectively. Fluorescence in the eluate was detected by a model RF-20A fluorescence detector (Shimadzu) with a 12-μL flow cell at the specific wavelength of excitation. A summary of detailed analytical conditions of the HPLC system is demonstrated in **Table 3.1**

HPLC-ICP-MS was also used to quantify SCN and SeCN, as shown schematically in **Figure 3.2**. The eluate was directly introduced into ICP-MS (Agilent 8800 Triple Quadrupole ICP-QQQ, Agilent Technologies, Hachioji, Japan). The observation of sulfur and selenium elements was operated by using the O_2 reaction mode, i.e., sulfur was detectable at m/z 48, and 50 ($^{32}S \rightarrow ^{32}S^{16}O+$ and $^{34}S \rightarrow ^{34}S^{16}O+$), and Se was detectable at m/z 94 and 96 ($^{78}Se \rightarrow ^{78}Se^{16}O+$ and $^{80}Se \rightarrow ^{80}Se^{16}O+$). The composition of the HPLC system containing a degassing unit (Gastorr AG-12, EverSeiko Corporation, Tokyo, Japan) and a pump for delivering the mobile phase (Hitachi L-2130, Hitachi High-Technologies

Corporation, Tokyo, Japan) A summary of detailed analytical conditions of the HPLC system demonstrated in **Figure 3.2**.

LOD and LOQ quantification based on calibration curves of HPLC-FLD and HPLC-ICP-MS

The LODs and the LOQs were expressed as follows.

$$LOD_{calibration} = 3.3 \times (\sigma/S)$$
 (Equation 1)

$$LOQ_{calibration} = 10 \times (\sigma/S)$$
 (Equation 2)

Where " σ " represents the standard deviation (SD) of the peak areas at the lowest concentration of the standard solution for three independent experiments, and "S" means the slope of the calibration curve.

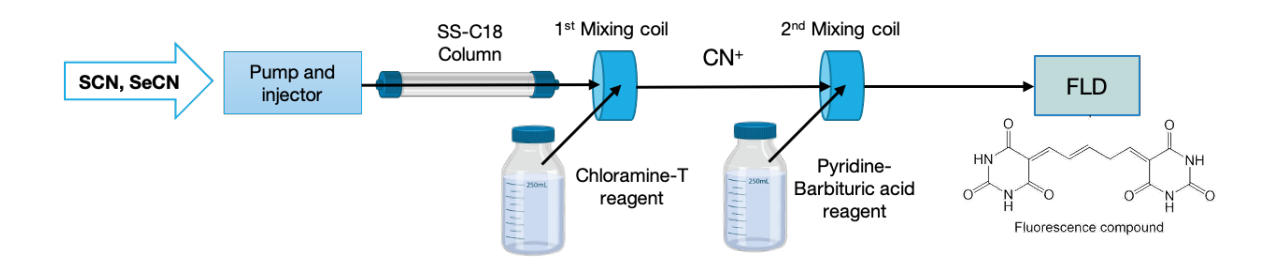


Figure 3.1. Scheme of HPLC-Fluorescence Detector (FLD) with post-column König reaction

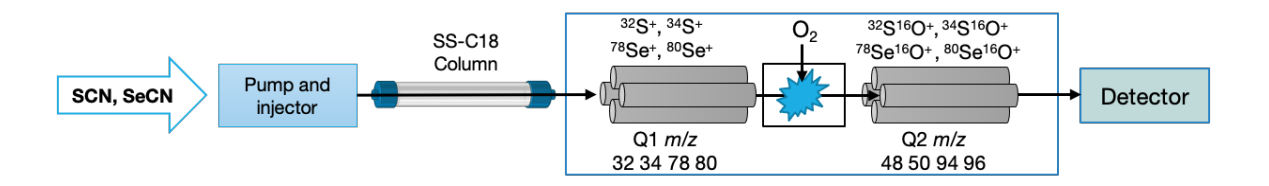


Figure 3.2. Scheme of HPLC-inductively coupled plasma mass spectrometer (HPLC-ICP-MS)

Table 3.1. HPLC conditions for HPLC-FLD with post-column König reaction

Reversed-phase HPLC column	Scherzo SS-C18 (3 μm, 4.6 i.d. x 250 mm with guard column)
HPLC mobile phase	0.1 M acetate buffer (pH 5.0) containing 12.5 mM sodium perchlorate/methanol (90/10, by volume), at the flow rate of 0.5 mL/min
Post-column reagent	

• Chloramine-T 0.1 w/v% chloramine-T solution, at the flow rate of 0.1 mL/min

Pyridine- barbituric acid	a mixture of 1.5 w/v% barbituric acid, 15% v/v% pyridine, and 3 v/v% concentrated hydrochloric acid, at the flow rate of 0.1 mL/min						
Wavelength	excitation 583 nm; emission 607 nm						
Injection volume	10 μL						
Column temperature	20–25°C						

Table 3.2. HPLC conditions for HPLC-ICP-MS

Reversed-phase HPLC column	Scherzo SS-C18 (3 μm, 4.6 i.d. x 250 mm with guard column)
HPLC mobile phase	0.1 M ammonium acetate (pH 5.0), at the flow rate of 0.7 mL/min
Injection volume	10 μL
Column temperature	20–25°C

Results and Discussion

The comparison of detection and separation of CN, SCN, and SeCN.

CN, SCN, and SeCN demonstrated the clear separation operated on a Scherzo SS-C18 column, and the determination of their fluorescence compound using the König reaction has been revealed (Figure 3.3). CN, SCN, and SeCN were eluted at 9.0, 11.8, and 14.1 min retention times, respectively. Although the peak of SeCN was slightly smaller than that of CN and SCN, the peak of SeCN was almost comparable to that of CN and SCN, indicating that the fluorescence-releasing derivatives of SeCN and SCN were parallelly active through König reaction. Completion of elution can be demonstrated within 20 min under specified elution conditions. The analysis results from HPLC-ICP-MS also showed that this is another method that can detect SCN and SeCN and can provide well segregation of targeted analytes results, as seen from its chromatogram (Figure 3.4). SCN and SeCN were eluted at 22.7 and 34.5 min retention times, respectively. ICP-MS detected sulfur and Se as part of the SCN and SeCN molecules, especially analytically, in the O₂ reaction mode.

However, we could observe that the elution conditions for HPLC-ICP-MS took twice as much time compared to the elution conditions for HPLC-FLD, indicating that SCN and SeCN were tightly bound in the Scherzo SS-C18 column. Because of the HPLC-ICP-MS elution, a high volume of methanol or organic solvents cannot be added to stabilize the

argon plasma. The absence of organic solvents further contributed stronger binding in the column of the targeted analytical substances, resulting in a slower retention time that took almost 45 min by HPLC-ICP-MS compared to HPLC-FLD for elution with broad peaks of SCN and SeCN. Therefore, no advantage of HPLC-ICP-MS over HPLC-FLD has been found in terms of qualitative analysis of SCN and SeCN.

According to the detection of our target analyte detection results between the two instrument systems used in these experiments, including, HPLC-FLD and HPLC-ICP-MS, it was initially found that the parameters of SCN and SeCN were directly comparable.

The comparison of sensitivity and linearity between HPLC-FLD and HLPC-ICP-MS

The establishment of SCN and SeCN calibration curves obtained from HPLC-FLD experiments was assessed in the concentration range of 0.01 to 10 μ M by triplicate injection of the aqueous standard solution mixture. The calibration curves obtained by HPLC-ICP-MS were assessed in the concentration range of 5 to 100 μ M for SCN and 1 to 100 μ M for SeCN, respectively. The summary of the analytical performance of HPLC-FLD with a post-column König reaction and HPLC-ICP-MS for SCN and SeCN determination is demonstrated in **Table 3.2**. The correlation coefficients for SCN and SeCN were 0.998 and 0.997, respectively. These parameters suggest the good linearity between signal intensities and concentrations of SCN and SeCN was obtained in the concentration range of 0.01 to 10 μ M SCN and SeCN by HPLC-FLD. Meanwhile, good linearities were observed for SCN and SeCN in the concentration range of 5 to 100 μ M and 1 to 100 μ M, respectively. It revealed that the correlation coefficients for SCN and SeCN were 0.990 and 0.998, respectively.

In addition to analyzing SCN and SeCN, HPLC-FLD can also provide the parameters of the CN analysis mentioned above. However, HPLC-ICP-MS cannot provide this analysis because CN is composed of carbon and nitrogen atom without metallic elements in the molecule. Good linearities were also observed for CN in the concentration range of 0.01 to 10 μ M only by HPLC-FLD, shown in **Table 3.3**. The correlation coefficient for CN was 0.990. This information shows another advantage over other instruments because HPLC-FLD can provide complete and simultaneous analysis of CN and their derivatives, such as SCN and SeCN. After that, both LOD and LOQ were calculated in the successive procedure.

The LOD and the LOQ for SCN obtained by HPLC-FLD with the post-column König reaction were 5.90 and 17.9 nM, and those for SeCN were 9.97 and 30.2 nM,

respectively (**Table 3.2**). HPLC-FLD with the post-column König reaction also provided the LOD for CN at 9.37 nM. On the other hand, the LOD and the LOQ for SCN obtained by HPLC-ICP-MS were 2.09 x 10³ and 6.33 x 10³ nM, whereas those for SeCN were 0.510 x 10³ and 1.55 x 10³ nM, respectively. The LOD for SCN indicated that HPLC-FLD was 354 times more sensitive than HPLC-ICP-MS (**Table 3.2**). Likewise, the LOD for SeCN indicated that HPLC-FLD was 51 times more sensitive than HPLC-ICP-MS. My HPLC-FLD method detected the fluorescence-emissive compound produced by the König reaction.

The König reaction can be quantitatively analyzed due to its specificity, especially for CN and its derivatives. Therefore, the determination of CN and its derivatives, SCN and SeCN, was frequently accomplished through this helpful reaction.

The emergency CN determination for the clinical setting for rapid treatment has been devised and evaluated by decreasing the extraction time of CN from the patient's blood sample. In this emergent measurement, the CN determination with König reaction is still considered the first choice (103).

The study of analytical methods for the simultaneous determination of CN and SCN in blood plasma and red cells of humans was developed and then performed by using the HPLC-FLD system with König reaction. Calibration curves derived from good linearity of blood CN and SCN were provided. They also apply this specified method of analysis to other clinical CN measurements, especially in smokers and non-smokers (28).

The measurement methods of CN have been developed that maintain the original concept of being simple, sensitive, specific and quantitative in blood and human body fluids for clinical and forensic applications. Other substances used in the concept of a König reaction were therefore selected, namely 2,3-naphthalenedialdehyde and taurine. In subsequent studies, CN and SCN could be quantitatively measured simultaneously using human blood as an assay. It was found to be very sensitive and highly accurate in testing (104).

In recent years, one significant study has developed a method for the determination of newly discovered CN derivatives, SeCN. It is the first study to establish the detection of CN derivatives in cell cultures confirmed by using the HPLC-FLD with König reaction in addition to CN and SCN, which are the primary metabolites of CN. It is shown that other derivatives, such as SeCN, can also react with the fluorescence-releasing compound similarly to CN and SCN. It was interesting that this published research can be further

developed and further studied on the biological circulation of CN derivatives in mammalian cells, even in negligible amounts (74).

According to the concept of König reaction, CN can be oxidized to cyanogen molecules by chloramine-T. The oxidization of SCN and SeCN can also be generated to produce (thio/seleno) cyanogen halides. Then the halides react with pyridine to establish glutaconaldehyde compounds that couple with barbituric acid (105). Therefore, the determination using a quantitively fluorometric method can perform by ascertaining intensely fluorescent emission (95).

On the other hand, ICP-MS helps analyze metal elements due to its susceptible and specific properties for metal atoms (40). ICP-triple quadrupole mass spectrometer was operated in this experiment according to the efficient elimination of molecular interference. It can offer higher sensitivity, rather than an ICP-single quadrupole mass spectrometer. However, the LOD and the LOQ for the quantification of SCN and SeCN obtained by HPLC-ICP-MS were inferior to those obtained by HPLC-FLD with the post-column König reaction. Sulfur and Se require a high ionization potential, i.e., sulfur and Se in argon plasma have relatively low ionization efficiencies compared with transition metals. These parameters provided by HPLC-ICP-MS indicated that it is not appropriate for the determination of sulfur and Se in the form of SCN and SeCN, respectively. HPLC-ICP-MS is time-consuming for one analysis compared to HPLC-FLD as HPLC-FLD with the post-column König reaction requires only 20 min, while HPLC-ICP-MS takes up to 45 min, suggesting a more appropriate technique for the quantification of SCN and SeCN is HPLC-FLD with the post-column König reaction.

The techniques used in this study were compared with previously reported techniques. The analytical parameters for quantifying SCN and SeCN, such as LOD, LOQ, and others, are summarized in **Table 3.5 and 3.6**, respectively. Various previous published studies have determined SCN and SeCN in biological fluids, wastewater, and forensic samples (99,106,107). Although my techniques are only applied to standard solutions. However, my techniques are only applied to standard solutions. However, the resulting analytical sensitivity was higher than previously reported techniques. Therefore, we applied my technique, in particular, HPLC-FLD, to the post-column König reaction to biological samples to reveal the suspected mechanisms underlying the biological transformation of SCN and SeCN.

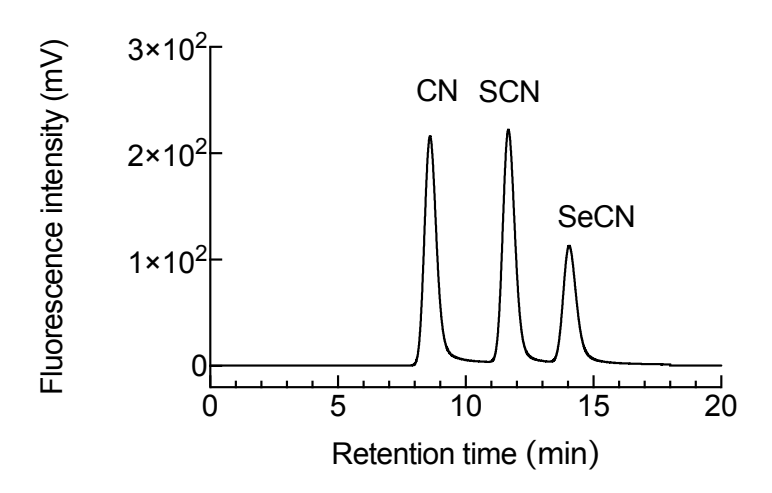


Figure 3.3. Elution profiles of 1.0 uM mixed standard solution of cyanide (CN), thiocyanate (SCN) and selenocyanate (SeCN) for HPLC-FLD with the post-column König reaction, a Scherzo SS-C18 column (3 μ m, 4.6 i.d. x 250 mm with a guard column) was isocratically eluted with 0.1 M acetate buffer, pH 5.0, containing 12.5 mM NaClO4/MeOH (90/10 v/v%). The eluate was reacted with König reagent and fluorescence was detected by the fluorescence detector at the excitation wavelength 583 nm and the emission wavelength of 607 nm.

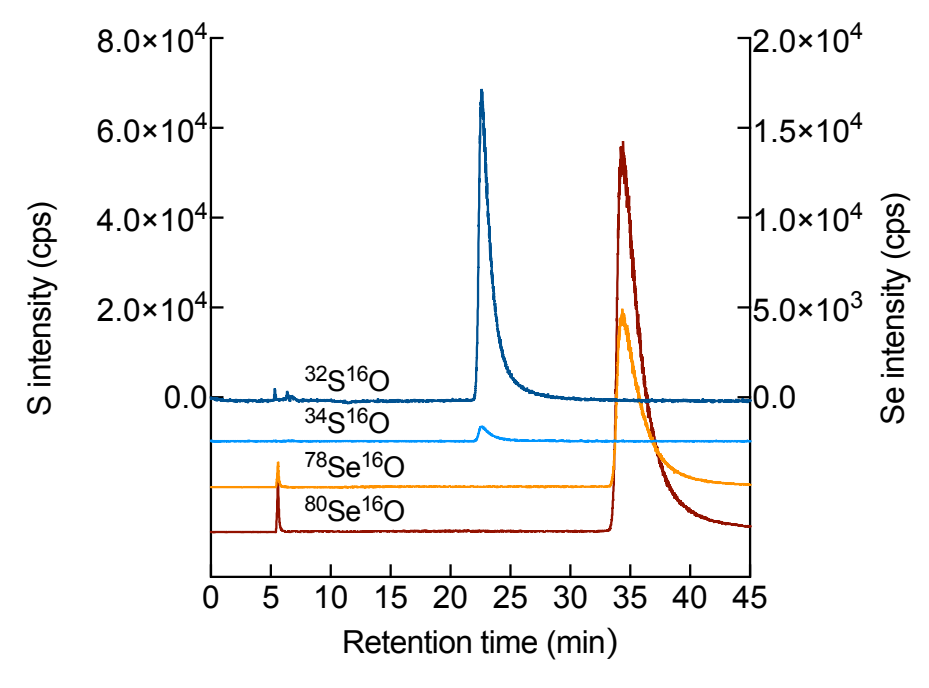


Figure 3.4. Elution profiles of 50 uM mixed standard solution of cyanide (CN), thiocyanate (SCN) and selenocyanate (SeCN) for HPLC-ICP-MS, a Scherzo SS-C18 column (3 μ m, 4.6 i.d. x 250 mm with a guard column) was isocratically eluted with 0.1 M ammonium acetate, pH 5.0. The eluate was directly introduced into ICP-MS/MS to monitor peaks at m/z 32 \rightarrow 48 for 32S (dark blue line), 34 \rightarrow 50 for 34S (light blue line), 78 \rightarrow 94 for 78Se (dark red line), and 80 \rightarrow 96 for 80Se (orange line).

Table 3.3. Parameters for HPLC-FLD with post-column König reaction and HPLC-ICP-MS for SCN and SeCN analysis.

Analytical technique	Analyte	Linear range (µM)	Equation of linearity curve	R^2	SD of peak areas of lowest calibrant	LOD (nM)	LOQ (nM)	Run time (min)
HPLC-FLD with	SCN	0.01-10	y = 1891865x - 1407	0.998	3385.98	5.90	17.90	20
post-column König reaction	SeCN	0.01-10	y = 1816663x - 140705	0.997	5490.14	9.97	30.22	20
HPLC-ICP-MS	SCN	5-100	y = 1842x + 6818	0.990	1166.60	2.09×10^{3}	6.33×10^{3}	35
	SeCN	1-100	y = 984.6x - 291.9	0.998	152.240	0.510×10^{3}	1.55×10^3	35

Table 3.4. Parameters for HPLC-FLD with post-column König reaction for CN analysis.

Analytical technique	Analyte	Linear range (µM)	Equation of linearity curve	R^2	SD of peak areas of lowest calibrant	LOD (nM)	LOQ (nM)	Run time (min)
HPLC-FLD with post-column König reaction	CN	0.01–10	y = 746756x + 49589	0.999	18547.73	9.37	28.38	20

Table 3.4. Comparison of parameters for analytical techniques for SCN analysis in various samples.

Analytical technique	Sample	Linear range	R^2	LOD	LOQ	Reference
HPLC-FLD with post- column König reaction	Standard solution	0.01–10 μΜ	0.998	5.90 nM	17.9 nM	Present study
HPLC-ICP-MS	Standard solution	5–100 μΜ	0.0990	$2.09\times10^3~\text{nM}$	$6.33 \times 10^3 \text{ nM}$	Present study
HPLC-FLD with 2-(4- carbazol-9-yl- benzylidene)- malononitrile (CMB) labeling	Swine plasma	0.01–3.7 μΜ	0.998	9.76 nM	12.3 nM	(96)
Ion-exchange chromatography - UV/VIS	Plasma, Urine	0–500 μΜ	1.00	$0.93 \times 10^3 \text{ nM}$	N.A.	(97)
UV/VIS	Plasma	25–500 μΜ	0.999	N.A.	$2.50 \times 10^3 \text{ nM}$	(98)
UV/VIS	Blood from deceased subjects	10.3–300 μΜ	0.999	$5.14 \times 10^3 \text{ nM}$	$10.3 \times 10^3 \text{ nM}$	(99)
IPC-UV	Water	$1.0 - 10 \times 10^3 \ \mu M$	0.990	$310 \times 10^3 \text{ nM}$	N.A.	(106)
GC-HRMS	Exhaled base condensate	0.01 nM–4 μM	0.998	5 nM	10 nM	(101)

Table 3.5. Comparison of parameters for analytical techniques for SeCN analysis in various samples.

Analytical technique	Sample	Linear range	R^2	LOD	LOQ	Reference
HPLC-FLD with post- column König reaction	Standard solution	0.01–10 μΜ	0.996	9.97 nM	30.2 nM	Present study
HPLC-ICP-MS	Standard solution	1–100 μΜ	0.998	$0.510\times10^3~\text{nM}$	$1.5 \times 10^3 \text{ nM}$	Present study
HPLC-FLD with König reaction	Standard solution, Blood, HEK293	0–10 μΜ	0.990	7.35 nM	24.5 nM	(74)
GC-MS/MS	Wastewater	0.3–100 ng/g Se	N.A.	0.1 ng/g Se	0.3 ng/g Se	(107)
ES-MS	Algae	N.A.	N.A.	0.12 nM	N.A.	(108)

CHAPTER 4

Simultaneous Detection of Thiocyanate and Selenocyanate in Living Mammalian Cells Including A549, HepG2, HEK293 and PC12 cells

Introduction

In the previous chapter, the detection and the analysis of intracellular SCN and SeCN in cells by HPLC-FLD with the post-column König reaction requires a clean sample preparation method. Sufficient clean samples can enhance the clear distinguishment for analyzing the target compounds peaks and separate them from the interference peaks from the biological complex matrices, especially in cell culture analysis samples. Although the König reaction is accurately specific to detecting CN and their derivatives, it can also react with other substances with carbon-nitrogen structure in the molecule, such as some amino acids, glycine (74,109), or acetonitrile (110).

The experimental results in the previous chapter demonstrated that HPLC-FLD with a post-column König reaction is a superior technique to HPLC-ICP-MS for the simultaneous detection of SCN and SeCN in terms of their sensitivity and shorter analysis time. The amount of SCN and SeCN in various mammalian cells, the potential organ representatives, exposed to selenite was quantified using the appropriate analytical technique, HPLC-FLD, with a post-column König reaction. The cytotoxic selenite attenuation by observing the biotransformation of SeCN and the association of intracellular SCN and SeCN were performed in this chapter.

Materials and Methods

Reagents

Sodium selenite, elemental form of selenium, was provided by Merck (Darmstadt, Germany). Acetone (guaranteed grade) was provided by FUJIFILM Wako Pure Chemical Corporation (Osaka, Japan). Trichloroacetic acid (Guarantee grade) was purchased from Nacalai Tesque (Kyoto, Japan). Phosphate buffered saline (PBS) was purchased from Sigma (St. Louis, MO, USA). Purified water was prepared by the Milli-Q system (Merck).

Cultured cells

Human lung carcinoma cell line, A549, and human hepatocellular carcinoma cell line, HepG2, were obtained from RIKEN Bioresource Center (Tsukuba, Japan). A549 and HepG2 were cultured and maintained in DMEM (Dulbecco's modified Eagle's medium;

Sigma) supplemented with 10% heat-inactivated fetal bovine serum (Biosera, Kansas City, MO, USA) and 1% penicillin-streptomycin mixed solution (Invitrogen, Carlsbad, CA, USA).

Rat adrenal pheochromocytoma cell line, PC12, was obtained from RIKEN Bioresource Center. PC12 was cultured and maintained in DMEM (Sigma) supplemented with 10% heat-inactivated fetal bovine serum (Biosera), 10% heat-inactivated horse serum (Culture Biologicals, Long Beach, CA, USA), and 1% penicillin-streptomycin mixed solution (Invitrogen).

Human embryonic kidney cell line, HEK293, was obtained from RIKEN Bioresource Center. HEK293 was cultured and maintained in MEM (modified Eagle's medium; Sigma) supplemented with 10% heat-inactivated fetal bovine serum (Biosera), 1% non-essential amino acid solution (Sigma), and 1% penicillin-streptomycin mixed solution (Invitrogen). All types of cells were maintained at 37°C under 5 v/v% CO₂ atmosphere. The cells were passaged after reaching confluence using 0.025 v/v% trypsin/EDTA in PBS (Fujifilm).

Measurement of selenite cytotoxicity

A549, HepG2, PC12, and HEK293 cells were separately seeded on 96-well plates at 1.0×10^5 cells/well and cultured for 24 h. The cells were exposed to 1.0, 2.5, 5.0, 10, 25, 50, 100, 250, 500, and 1,000 μ M sodium selenite in FBS-free DMEM or MEM for 24 h. After the treatment, 20 μ L of MTS reagent (3-(4,5-dimethylthiazol-2-yl)-5-(3-carboxymethoxyphenyl)-2-(4-sulfophenyl)-2H-tetrazolium, CellTiter 96® AQueous One Solution (Promega, Madison, WI, USA) was added and the cells were incubated for 1 h at 37°C. Then, the absorbance at 490 nm in each well was measured by a microplate reader (Molecular Devices, San Jose, CA, USA).

Selenite exposure and sample preparation for SCN and SeCN detection

A549, HepG2, PC12, and HEK293 cells were separately seeded on 60 millimeters plates at 1.0×105 cells/ml and cultured up to 72 h, and then divided into two groups. One group was exposed to sodium selenite at two non-toxic concentration levels for each cell type obtained from the cytotoxicity tests. The other group served as control. A549, HepG2, and PC12 cells were incubated with 2.5 and 5 μ M sodium selenite, and HEK293 cells were incubated with 1 and 2.5 μ M sodium selenite for 24 h. Subsequently, the cells were collected with a 250- μ L aliquot of cold 0.5x PBS, and the number of collected cells was

counted. The suspended cells were homogenized with an ultrasonic homogenizer (Bioruptor®, Bio-Rad, Japan) on ice at 200 W, 20 kHz three times each for 30 s at 30-s intervals. To remove sample protein, A 200-µL aliquot of ice-cold acetone was added to the same volume of cell homogenates, the sample mixture was gently mixed and then left for 10 min. The sample mixture was centrifuged at 15,000g for 15 min at 4°C. The supernatant was collected and gently mixed with 200 µL of 0.1 M bicarbonate buffer, pH 10.0 to stabilize SCN and SeCN. The solution was filtered through a 0.2-µm Millex-LH membrane filter (Millipore, Darmstadt, Germany). A 20-µL aliquot of the filtrate was injected into the HPLC-FLD. Each experiment was repeated three times.

The recovery of this extraction method will also be evaluated from the peak areas of SCN and SeCN standard solution depend on the process of sample preparation compared to direct analysis of SCN and SeCN standard solution at $0.5~\mu M$ as a low concentration and $5~\mu M$ as a high concentration on the calibration curve, respectively. In addition, to determine intracellular SCN and SeCN concentrations, the SCN and SeCN stock solutions were diluted with 0.5x~PBS, pH 7.4 to prepare working mixed standard solutions having concentrations of 0.050, 0.10, 0.50, 1.0, 2.5, and $5.0~\mu M$.

Statistical analysis

Following HPLC-FLD post-column König reaction analysis, the data analysis was performed by Prism GraphPad 9.0.0 software (GraphPad Software Inc., La Jolla, CA, USA) and Microsoft 365 Excel (Microsoft Corporation, Redmond, WA, USA). Values are shown as means \pm SD. Dunnett's multiple comparisons test was used to evaluated data. The establishment of significant difference was set at p < 0.05.

Results and Discussion

The efficacy of extraction for SCN and SeCN between trichloroacetic acid and acetone

The detection and analysis of intracellular SCN and SeCN in cells by HPLC-FLD with the post-column König reaction requires a pretreatment method so that the peaks of the target compounds should be clearly separated from the interference peaks originating from the biological matrices, especially in cultured cells. Although the König reaction was accurately specific to the detection of CN and their derivatives, i.e., SCN and SeCN, it also reacted with other substances having a carbon-nitrogen structure in its molecule such as glycine (74,109) and acetonitrile (110). Cultured mammalian cells consist of complex matrices that may interfere with SCN and SeCN detection by HPLC-FLD with the post-

column König reaction. I, therefore, eliminated the interfering peaks by the most widely used method of extraction, i.e., the protein precipitation. The technique has been applied to the extraction of SCN in biological samples by acids or organic solvents. It was also effective to stop the reaction that may interfere with the experiments.

To evaluate the extraction efficacy and the effect on the retention times of CN, SCN, SeCN standards, ice-cold 12.5% TCA and 50% acetone were tested. The TCA-precipitation found the retention time shifts of SCN and SeCN (**Figure 4.1**). Although the average extraction efficacy of CN increased, that of SeCN was decreased. The percent of relative standard deviations (%RSDs) of CN and SeCN were unacceptable in terms of reproducibility. It was suspected that high concentration of TCA caused the degradation of SeCN, and a part of SeCN was decomposed back to CN. On the other hand, 50% acetone showed the better extraction efficiency of SCN and SeCN than TCA. The recovery of SCN and SeCN at the lower (0.5 μ M) and the higher (5 μ M) concentrations were 99.4±5.7% and 107±10%, and 95.0±7.8% and 103±9.7%, respectively. The %RSDs and recoveries were summarized in table. These results indicated that 50% acetone gave me more acceptable reproducibility and higher precision for SCN and SeCN than 12.5% TCA (**Table 4.1**). Therefore, the pretreatment with 50% acetone was applicable to the detection of SCN and SeCN in living cells.

As a sample pretreatment for intracellular analysis of SCN and SeCN, acetone allowed me to detect SCN and SeCN. I obtained good separation under the matrix-free condition and in the presence of biological matrices. At least, the matrices affecting the separation of SCN and SeCN could be removed by the acetone treatment. Initially, 12.5% TCA was chosen for the protein precipitation step because it is a convenient and conventional method for sample preparation by denaturation and the precipitation of proteins. Indeed, several studies described the determination of SCN in blood, urine, or milk by TCA as a precipitating protein agent (111,112), and showed the analytical results with precision and accuracy. My results were consistent with these preceding studies in terms of accuracy by the pretreatment with TCA. However, the precision obtained by the area under the peak was less reliable at low, 0.5 μ M, and high 5.0 μ M concentrations. Moreover, SeCN could be acid-susceptible due to the loss of stability of SeCN by the acid extraction process. As mentioned, the peak of SeCN became small by the acid treatment, and the treatment increased the peak of CN, suggesting the SeCN degradation and the release of CN.

Organic solvents are also widely used for protein precipitation. Methanol is one of the frequently used organic solvents for protein precipitation. However, it could not separate the targeted peaks from the interference peaks of other substances in the cell culture. Acetone is also used for protein precipitation and is applied to electrospray ionization (ESI), time of flight (ToF), or ion trap mass spectrometry (113). Acetonitrile (ACN) is another water-miscible organic solvent and is also used for protein precipitation (114). However, acetone should be preferred over ACN because ACN can react with the 1st and 2nd post-column reagents in HPLC-FLD with the post-column König reaction. Thus ACN may interfere with the detection of SCN and SeCN. Moreover, because the acetone treatment also improved the extraction efficiency of SCN and SeCN, acetone could stabilize SCN and SeCN through the pretreatment.

The determination of SCN and SeCN in biological matrices

According to the results of the experiments using standard compounds, I applied the pretreatment method to cultured cell matrices. The supernatant of HepG2 cells was spiked with SCN and SeCN authentic standards for the analysis by HPLC-FLD with the post-column König reaction. The elution profile of the unspiked sample showed that biological matrices were eluted before 11 min and wholly separated from endogenous SCN (**Figure 4.2A**). In the elution profile of the spiked sample, SCN and SeCN were well separated even in the presence of biological matrices (**Figure 4.2B**). The linearities between signal intensities and the concentrations of SCN and SeCN were maintained over the concentration range of 0.05 to 5 μ M (**Table 4.2**). The correlation coefficients for SCN and SeCN were 0.993 and 0.985, respectively.

However, this technique has not accomplished the detection of intracellular CN in this experiment due to enormous matrix peaks overlapping with the retention time corresponding to CN ion. To more clearly and specifically detect CN, the pretreatment conditions should be more carefully evaluated in future studies.

The cytotoxicity of selenite and the determination of SCN and SeCN in four mammalian cell lines

The developed method was used to quantify the total amounts of intracellular SCN and SeCN in cultured cells. Cytotoxicity tests were performed to evaluate the detoxification of selenite in the cells. Selenite showed cytotoxicity in four mammalian cell lines, A549, HepG2, PC12, and HEK293at the various concentration from 0.1 to 1,000 µM (**Figure 4.3**).

The cytotoxicity test indicated that A549 was the most tolerant cell line, followed by HepG2 and PC12. HEK293 was more sensitive than the other three cell lines. Each cell line was exposed to selenite at the non-toxic dose according to the results of the preceding cytotoxicity test. The intracellular concentrations of SCN and SeCN were determined. As expected, the most sensitive to selenite among the cell lines was HEK293. Thus, selenite was exposed at 1.0 and 2.5 μM to HEK293 and at 2.5 and 5.0 μM to the other three cell lines. The typical chromatograms are shown in **Figure 4.4**. Endogenous SCN, but not endogenous SeCN, was detected in all cell lines. SeCN was detected in all cell lines when selenite was exposed (**Figure 4.4B, C, E, F, H, I, K, and L**). The selenite exposure significantly increased total intracellular SCN and SeCN concentrations in A549, HepG2, and PC12. In particular, A549 and HepG2 more efficiently generated intracellular SCN and SeCN than PC12. Meanwhile, no significant difference in total intracellular SCN and SeCN concentrations was observed in HEK293 exposed to selenite (**Figure 4.5**).

Compared with their intact cells, a significant increase in total amounts of intracellular SCN and SeCN was found in selenite-exposed A549, HepG2, and PC12 cells. Meanwhile, there were no differences in total amounts of intracellular SCN and SeCN in HEK293 between the selenite-exposed and control groups. I speculated that there were differences in the capacity of endogenous CN among the cell lines. Selenite, Se(+IV), is quickly reduced to selenide, Se(-II), in vivo. Selenide seems to induce the production of endogenous CN, and then endogenous CN reacts with selenide. Several studies have also indicated that selenite can accelerate the generation of superoxide anion (115–119). As mentioned above, selenite is reduced to selenide and selenide can reduce oxygen to produce reactive oxygen species such as superoxide anion (120–122). Therefore, selenite was able to efficiently stimulate intracellular CN production via oxidative stress mediated by reactive oxygen species. As a result, this process could lead to an increase in intracellular concentrations of SCN and SeCN. The differences in total SCN and SeCN concentrations among cell lines indicated the differences in the metabolic capacity for the production of endogenous CN. Additional studies are necessary to elucidate the factors determining metabolic capacity, e.g., the enzyme(s) responding to the endogenous CN metabolism and the production of CN precursors in the cells.

Endogenous SCN was also detected in all cell lines without selenite exposure. Then, it decreased with the increase in the selenite concentration of exposure, indicating that SeCN was competitively generated with SCN. In addition, the selenite treatment could induce CN, as abovementioned. Endogenous SCN was coupled between endogenous CN

and reactive sulfur species, i.e., sulfane sulfur. In detail, endogenous CN more preferably reacted with selenide than sulfane sulfur. Because the SeCN formation was accomplished non-enzymatically by a rapid chemical reaction between endogenous CN and selenide, it was reported that SCN was rapidly excreted into urine and saliva from the bloodstream (100,123), and did not accumulate in tissue (124). On the other hand, SeCN was pooled in mammalian cells and was utilized as a source of Se (40). These observations suggest the biological significance of SeCN was different from that of SCN.

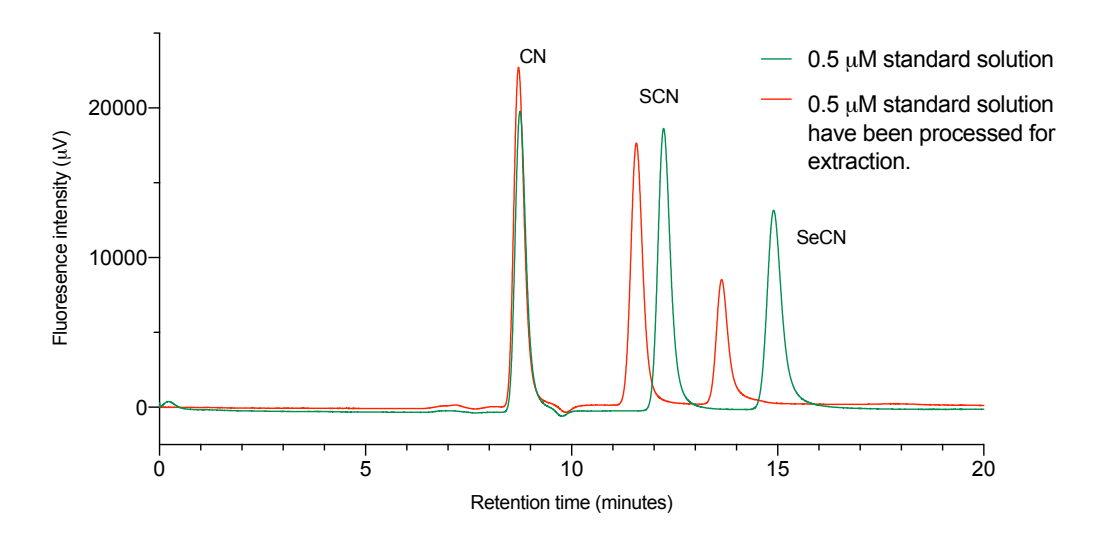
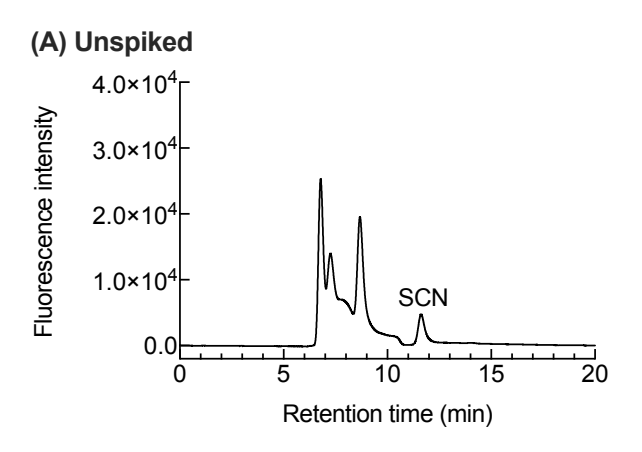


Figure 4.1. The retention time between 0.5 μ M CN, SCN, and SeCN standard mixture and 0.5 μ M standard mixture (green line) and standard mixture have been processed for extraction by using TCA (red line)



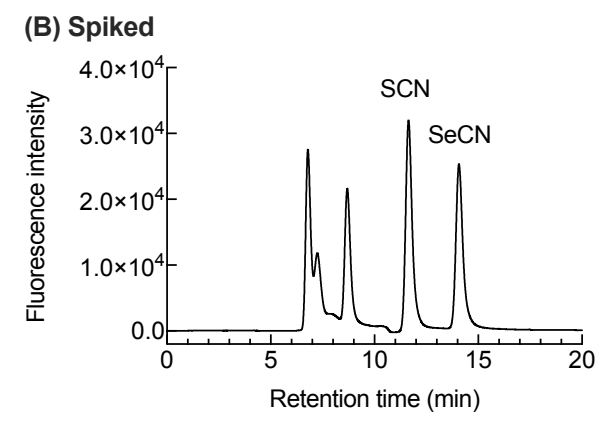


Figure 4.2. Elution profiles of HepG2 supernatant obtained by HPLC-FLD with the post-column König reaction. The HepG2 supernatant that was not spiked (A) or spiked (B) with SCN and SeCN mixed standard solution was applied to a Scherzo SS-C18 column (3 μ m, 4.6 i.d. x 250 mm with a guard column), and isocratic elution was carried out with 0.1 M acetate buffer, pH 5.0, containing 12.5 mM NaClO4/MeOH (90/10 v/v%). The eluate was reacted with König reagent and fluorescence was detected by the fluorescence detector at the excitation wavelength of 583 nm and the emission wavelength of 607 nm.

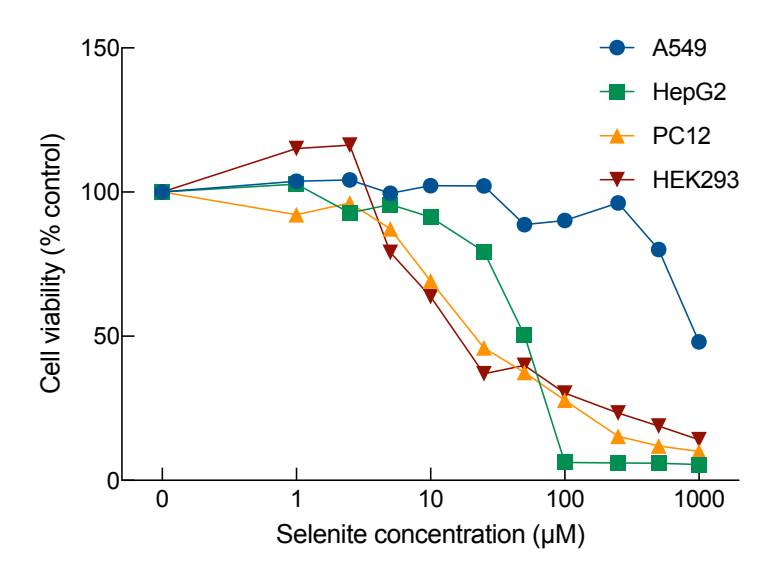


Figure 4.3. Cytotoxic effect of four cell lines exposed to various concentrations of sodium selenite. A549, HepG2, PC12, and HEK293 cells were exposed to 0, 1.0, 2.5, 5.0, 10, 25, 50, 100, 250, 500, and 1000 μ M sodium selenite in FBS-free DMEM for 24 h. Cell viability was determined by MTS assay. Each point represents data from three separate experiments.

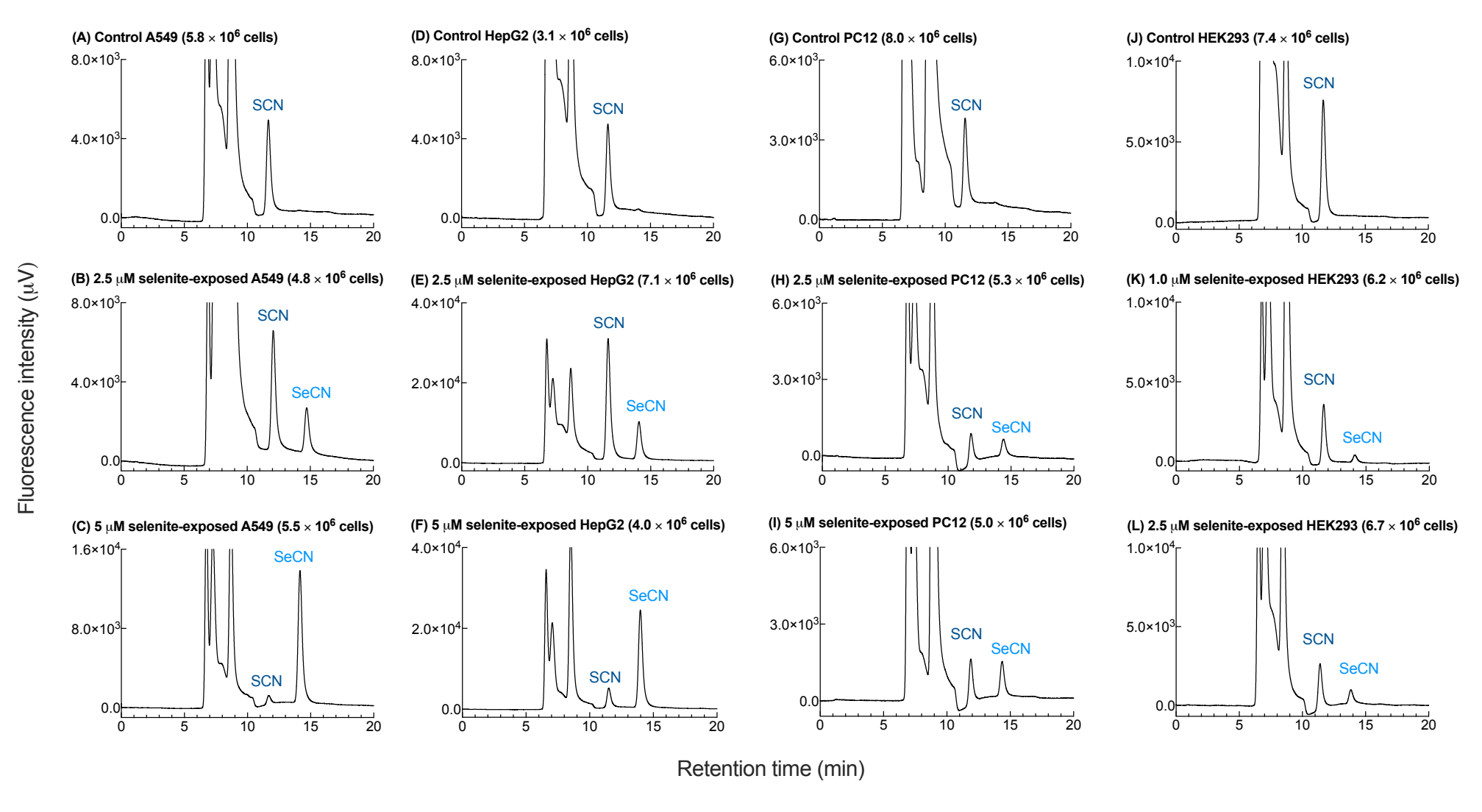


Figure 4.4. Detection of intracellular SCN and SeCN concentrations in selenite-exposed A549, HepG2, PC12, and HEK293. The number of cells in each experiment is shown in parentheses.

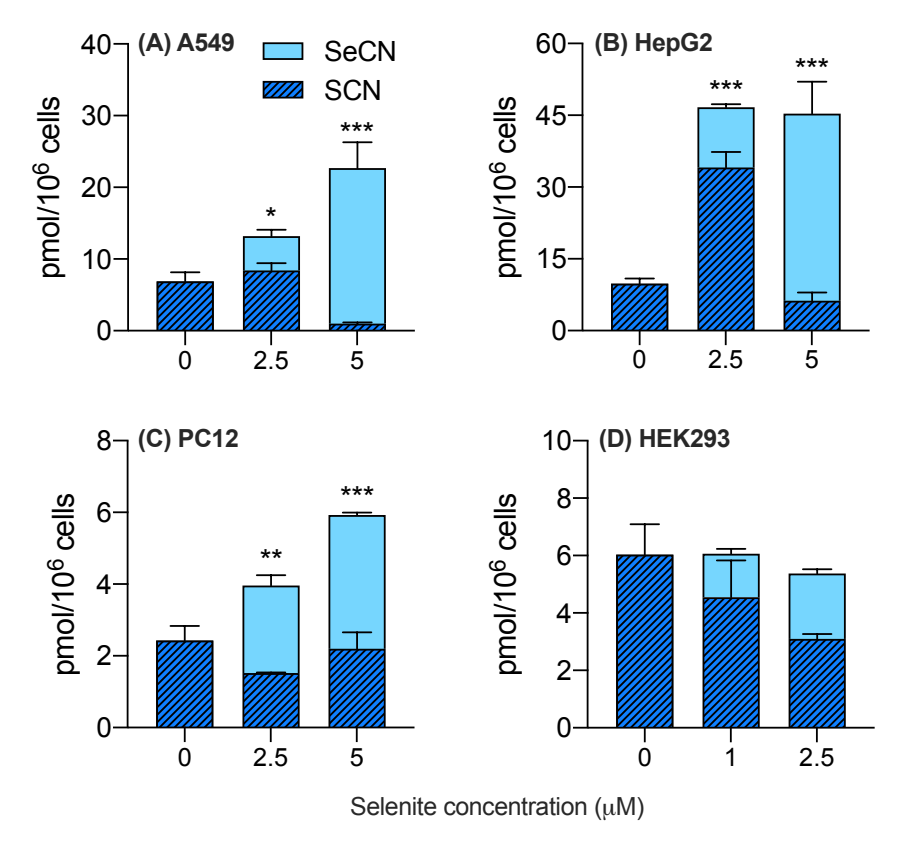


Figure 4.5. Total intracellular SCN and SeCN concentrations in A549 (A), HepG2 (B), PC12 (C), and HEK293 (D) cells exposed to selenite and control cells. Means \pm SD represent data from three separate experiments. (*p < 0.05, **p < 0.01, ***p < 0.001)

Table 4.1. Extraction efficacy and %RSD for SCN and SeCN standard mixture in 50 mM PBS for liquid extraction method compared between using ice-cold TCA and acetone.

Protein Precipitating Agent	Analyte	Standard concentration (µM)	Extraction efficacy (%)	%RSD	
12.5% TCA	CON	0.5	83.52	4.960	
	SCN	5.0	101.9	1.420	
	G GN I	0.5	54.99	12.84	
	SeCN	5.0	89.81	4.17	
50% Acetone	CC) I	0.5	99.44	5.715	
	SCN	5.0	107.3	10.62	
	G G2.I	0.5	95.03	7.836	
	SeCN	5.0	102.8	9.739	

Table 4.2. Parameters for HPLC-FLD with post-column König reaction for intracellular SCN and SeCN analysis.

Analytical technique	Analyte	Linear range (µM)	Equation of linearity curve	R^2	SD of peak areas of lowest calibrant	LOD (nM)	LOQ (nM)	Run time (min)
HPLC-FLD with post-column König reaction	SCN	0.05-5	y = 662356x + 2644	0.993	1202.68	5.99	18.2	20
	SeCN	0.05-5	y = 596434x - 21363	0.985	800.500	4.43	13.4	20

CHAPTER 5

Effect of Myeloperoxidase on Intracellular Thiocyanate and Selenocyanate Generation

Introduction

It has been reported that endogenous CN is detected in neurons exposed to hydrogen peroxide, and it seems that the mechanism of intracellular CN production is related to oxidative processes (125). Endogenous CN in neutrophils by MPO (17). I speculated that hydrogen peroxide could contribute to the production of endogenous CN similar to neuronal cells and neutrophils. Based on the experimental results in the previous chapter, intracellular CN was proposed to play an important role in attenuating selenium toxicity, although CN itself is well known to be highly toxic substant. This chapter evaluated one of the key mechanisms involved in producing endogenous CN in mammalian cells.

MPO catalyzes the redox reactions that can cause severe tissue damage during inflammation. Some previous studies suggest that MPO is a crucial enzyme to produce endogenous CN, i.e., hypochlorous acid (HOCl), a well-known strong cytotoxic oxidant produced by MPO is required to produce endogenous CN. HOCl oxidizes glycine, and the cyanogen chloride (CNCl) is generated via chlorination under acidic conditions. This CNCl is metabolically equal to endogenous CN.

MPO is a highly expressed enzyme in neutrophils, and a human leukemia cell line, HL60, expresses MPO. Since previous studies indicate that MPO accelerated endogenous CN production, so HL60 could more efficiently produce SCN and SeCN from endogenous CN compared to another leukemia cell line, K562, which did not express MPO (17,125). In the previous chapters, I revealed that intracellular SCN and SeCN were well-detected and quantified by HPLC-FLD with the post-column method. In this chapter, HL60, K562, and the human hepatocarcinoma cell line, HepG2, were used to demonstrate the mechanisms for the production of endogenous CN. was widely observed in mammalian To clarify the role of MPO in endogenous CN production. The MPO inhibitor, AZD3241, was used to assess the intracellular biotransformation of SCN and SeCN.

Materials and Methods

Reagents

Sodium selenite was provided by Merck (Darmstadt, Germany). Acetone (guaranteed grade) was provided by FUJIFILM Wako Pure Chemical Corporation (Osaka,

Japan). Phosphate buffered saline (PBS) was purchased from Sigma (St. Louis, MO, USA). MPO inhibitor, AZD 3241, was provided by Selleckchem (Houston, TX, USA). Purified water was prepared by the Milli-Q system (Merck).

Cultured cells

Human leukemia cells including, promyeloblast cell line, HL60, and lymphoblast cell line, K562, and were obtained from RIKEN Bioresource Center. HL60 and K562 cells were cultured and maintained in in RPMI-1640 (Roswell Park Memorial Institute 1640 medium; Sigma) supplemented with 10% heat-inactivated fetal bovine serum (Biosera), and 1% penicillin-streptomycin mixed solution (Invitrogen). All types of cells were maintained at 37°C under 5 v/v% CO₂ atmosphere. The cells were passaged after reaching confluence.

Measurement of selenite cytotoxicity

24 h cultured HL60 and K562 cells were separately seeded on 96-well plates at 1.0 \times 10⁵ cells/well. The cells were incubated with 1.0, 2.5, 5.0, 10 ,25, 50, 100, 250, 500, and 1,000 μM sodium selenite in FBS-free RPMI-1640 for 24 h. After the treatment, 20 μL of MTS reagent (3-(4,5-dimethylthiazol-2-yl)-5-(3-carboxymethoxyphenyl)-2-(4-sulfophenyl)-2H-tetrazolium, CellTiter 96® AQueous One Solution was added, and the cells were incubated for 1 h at 37°C. Then, the absorbance at 490 nm in each well was measured by a microplate reader. The highest non-toxic dose for HepG2 from the cytotoxicity test in the previous topic was used in this assay at 5.0 μM.

Pretreatment with MPO inhibitor and selenite exposure

To determine the cytotoxic effect of selenite, human leukemia cells HL60 and K562 cells were separately seeded in 50 milliliters cell culture flask. In contrast, HepG2 cells were maintained on 60 millimeters plates at 1.0×10^5 cells/ml, cultured for up to 72 h, and then divided into two groups for each cell line. Two different experimental conditions of the pretreatment were assessed, including 24 hours RPMI-1640 medium incubation for human leukemia cells and DMEM incubation for HepG2 cells as a control group. 24 hours AZD-3241 each suitable culture medium incubation as MPO inhibitor-pretreated group.

Subsequently, pretreated cultured cells were exposed to sodium selenite at the highest non-toxic concentration levels as 1 μ M for human leukemia cells, and pretreated HepG2 cells were exposed to 5 μ M for 24 hours. Then, the cells were collected to perform

sample preparation in the same procedure as the previous chapter for the intracellular SCN and SeCN quantification. MPO inhibitor, AZD3241, was selected at $15\mu M$ in the cultured medium. These concentrations were taken from the previously published in vitro experiments in which MPO inhibitor is expected to inhibit the entire activity of MPO or other possibly existing enzymes with similar properties (126). Each experiment was repeated three times.

Results and Discussion

Effects of myeloperoxidase inhibitor on SCN and SeCN production

The selenite exposure cytotoxicity tests in the leukemia cell lines, HL60, and K562 cells were performed. Then, cytotoxic characteristics of selenite sensitivity for each cell type were revealed. The total amounts of intracellular SCN and SeCN in the cells were quantified in selenite/MPO inhibitor-exposed cells. The cell type-specific cytotoxicity of selenite was observed at the concentration from 0.1 to 1,000 µM (Figure 5.1). Both cell lines were susceptible to selenite. However, K562 was more susceptible to selenite at a lower concentration of less than 10 µM. Then, the intracellular concentrations of SCN and SeCN were determined. HL60, K562, and HepG2 cells were pretreated with AZD3241 for 24 hrs, and then three cell lines were exposed to sodium selenite at the highest non-toxic concentration levels for additional 24 hrs. The maximum non-toxic concentration level of selenite was 1.0 µM for two leukemia cell lines. For HepG2 cells, the highest non-toxic concentration level was 5.0 µM. Then, the determination of intracellular SCN and SeCN concentrations was performed by HPLC-FLD with the post-column König reaction. Intracellular SCN and SeCN can be detected by HPLC-FLD and shown in the typical chromatogram in (Figure 5.2). These data provided that SeCN was generated in both leukemia cell lines exposed to selenite.

As shown in **Figure 5.3**, the MPO inhibitor, AZD3241, significantly decreased the amounts of intracellular SCN and SeCN in all cell lines, i.e., HL60, K562, and HepG2 cells. The amount of thiocyanate measured in HL60 cells showed that 3.92±0.147 pmol/10⁶ cells decreased to 2.03±0.233 pmol/10⁶ cells, 6.44±1.24 pmol/10⁶ cells declined to 4.21±0.258 pmol/10⁶ cells for K562 cells, and 11.3±1.86 pmol/10⁶ cells was dramatically reduced to 3.79±0.790 pmol/10⁶ cells for HepG2 cells between the control group and AZD3241 pretreat groups. At the same time, the reduction in the amount of SeCN measured in cells was shown to be 2.83±0.741 pmol/10⁶ cells to 0.167±0.0341 pmol/10⁶ cells for HL60 cells, 5.22±1.052 pmol/10⁶ cells to 2.66±0.265 pmol/10⁶ cells for K562 cells, and 37.3±2.34

pmol/ 10^6 cells to 18.2 ± 3.09 pmol/ 10^6 cells for HepG2 cells, between the control group and AZD3241 pretreat groups.

The inhibition in HL60 was easily explainable because HL60 was expressing MPO. However, the inhibitory effect of AZD3241 was also observed in K562 and HepG2. Since these cell lines were known not to express MPO, it seemed challenging to explain the effect of AZD3241. I speculated that endogenous CN could be generated by an MPO-like enzyme inhibited with AZD3241. Several studies have described possible enzymes involved in the formation of CN within living organisms through various redox reactions. Namely, several peroxidase family enzymes are feasible enzymes to produce endogenous CN in MPO-non-expressing cells. Lactoperoxidase has a similar activity to myeloperoxidase, which can convert SCN to CN and sulfate (127). Thyroid peroxidase also has a similar activity (128). The conversion of SCN can proceed through the enzymatic reaction by acid-catalyzed oxidation with H₂O₂ in erythrocytes (129). The identification of a putative enzyme(s) with an MPO activity should be performed in future sequencing studies, and then, the inconclusive mechanism of endogenous CN generation is expectedly revealed after the identification.

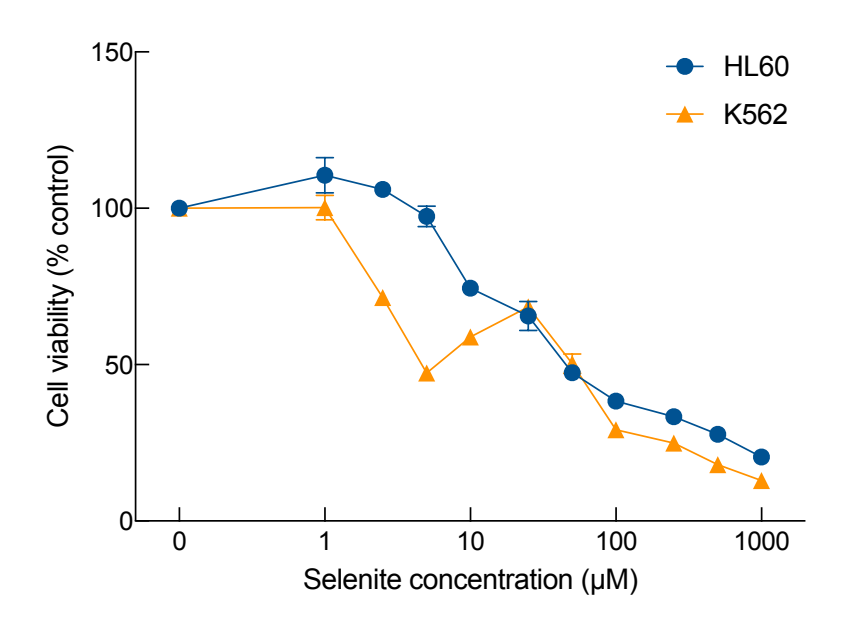


Figure 5.1. Cytotoxic effect of four cell lines exposed to various concentrations of sodium selenite. HL60 and K562 cells were exposed to 0, 1.0, 2.5, 5.0, 10, 25, 50, 100, 250, 500, and 1000 μ M sodium selenite in FBS-free RPMI-1640 for 24 h. Cell viability was determined by MTS assay. Each point represents data from three separate experiments.

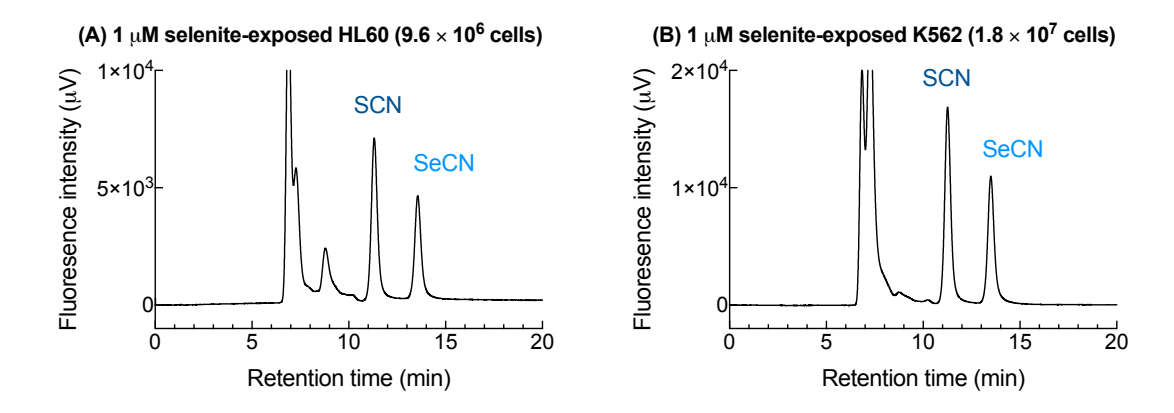


Figure 5.2. Detection of intracellular SCN and SeCN concentrations in selenite-exposed HL60 and K562 cells. The number of cells in each experiment is shown in parentheses.

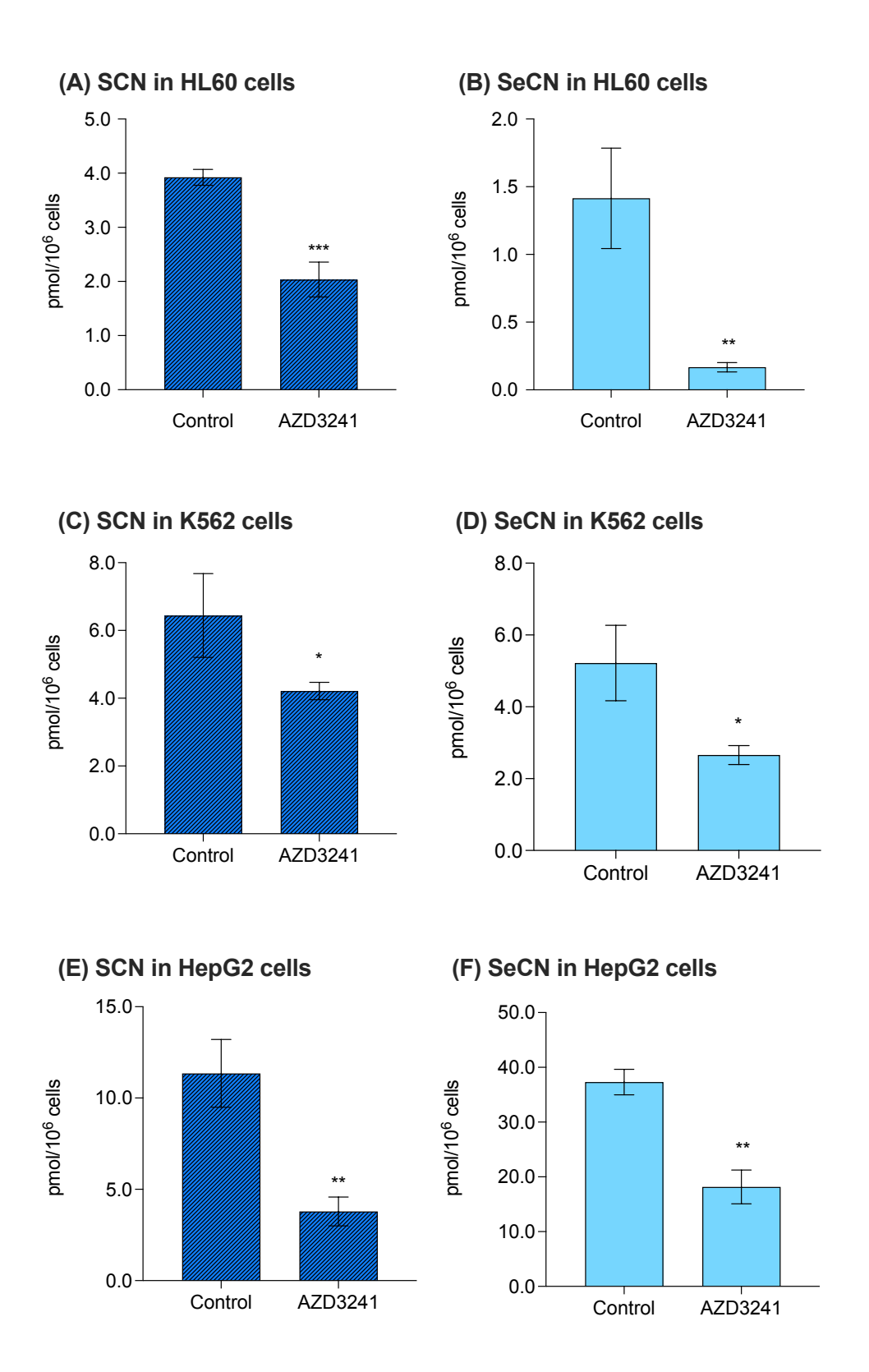


Figure 5.3. Total intracellular SCN (A, C, E) and SeCN (B, D, F) concentrations in selenite-exposed HL60, K562, and HepG2 cells, respectively, pretreated with myeloperoxidase (MPO) inhibitor, AZD324, and control cells. Means \pm SD represent data from three separate experiments. (*p < 0.05, **p < 0.01, ****p < 0.001)

CHAPTER 6

Conclusion

Comparison of quantification of thiocyanate (SCN) and selenocyanate (SeCN) between HPLC-Fluorescence Detector (HPLC-FLD)) with post-column König reaction and HPLC-inductively coupled plasma mass spectrometer (HPLC-ICP-MS) were studied in terms of sensitivity and linearity. The operation of the HPLC-FLD system with a postcolumn König reaction using Scherzo SS-C18 column provided the clear separation of cyanide (CN), SCN, and SeCN in the standard solution mixture eluted at 9.0, 11.8, and 14.1 min retention times, respectively. The elution can accomplish in 20 minutes. HPLC-ICP-MS system under the same column also gave the SCN, and SeCN separation eluted at 22.7 and 34.5 min retention times, respectively, with a more extended period than the HPLC-FLD system. The correlation coefficients for SCN and SeCN obtained from both systems were excellent at 0.998 and 0.997, respectively, by HPLC-FLD. HPLC-ICP-MS provided at 0.990 and 0.998, respectively. Only HPLC-FLD can detect CN with a correlation coefficient of 0.990. The limit of detection (LOD) for SCN indicated that HPLC-FLD was 354 times more sensitive than HPLC-ICP-MS. Meanwhile, the LOD for SeCN indicated that HPLC-FLD was 51 times more sensitive than HPLC-ICP-MS. HPLC-FLD is, therefore, the most appropriate analytical technique with superior sensitivity and shorter analysis time for simultaneous analysis of SCN and SeCN compared to HPLC-ICP-MS.

The amounts of SCN and SeCN in various mammalian culture cells, including A549, HepG2, PC12, and HEK293, exposed with selenite were quantified. It reveals the detoxification of selenite by its biotransformation to SeCN. The four types of cultured mammalian cells representing essential organs were exposed to sodium selenite for 24 hours at two non-toxic concentrations for each cell type provided by the cytotoxicity tests. The cell sample preparation was performed and analyzed, including intracellular SCN and SeCN. The usefulness of ice-cold acetone in the deproteinization step yielded a markedly improved SCN and SeCN extraction efficiency compared to the trichloroacetic acid (TCA) with the constant retention time and the excellent stability of the targeted substance to be analyzed above. HPLC-FLD with the post-column technique provided a good separation of SCN and SeCN spiked in the biological matrices by the pretreatment of ice-cold acetone as a deproteinizing agent. However, this technique cannot detect intracellular cyanide due to enormous matrices peaks overlapping with the retention time corresponding to cyanide ions. Future subsequent studies to detect cyanide more clearly and specifically should

emphasize the pretreatment conditions. HPLC-FLD also provided simultaneous detection of endogenous SCN and SeCN in living mammalian cells deproteinized by acetone. SeCN was detected in all cell lines when selenite was exposed. The selenite exposure significantly increased total intracellular SCN and SeCN concentrations in A549, HepG2, and PC12.

Meanwhile, no significant difference in total intracellular SCN and SeCN concentrations was observed in HEK293 exposed to selenite. In all cell lines, SCN concentration decreased with increased selenite concentration, suggesting that SeCN was competitively generated with SCN. The selenite-tolerant cell lines such as A549, HepG2, and PC12 can induce endogenous CN to form SCN and SeCN noted by the increased total amount of target metabolites. Selenium and sulfur seemed to be competitively transformed into SeCN and SCN. A higher concentration of intracellular SeCN generated non-enzymatically from endogenous CN combined with selenide species was produced more than SCN. These results provide that endogenous CN is one of the detoxification factors for selenite toxicity. SeCN was more likely to be deposited in cells than SCN.

The effect of myeloperoxidase (MPO) on intracellular cyanide production was evaluated by observing the determination of SCN and SeCN. MPO inhibitor AZD-3241 was used to pretreat cultured cells and followed the targeted substance. The HL60 cell line with a definite presence of MPO enzymes involved in endogenous CN formation was used to study the biotransformation of SCN and SeCN in mammalian cell types compared with K562 cultured mammalian lymphocytes as a negative control. HepG2 cell was also evaluated. These cells were incubated with 24 hours AZD-3241, exposed to selenite, and ultimately determined intracellular SCN and SeCN. AZD3241 significantly decreased the amounts of intracellular SCN and SeCN in all cell lines. It suggested that MPO can affect the intracellular production of SCN and SeCN from the result of HL60 cells. However, the inhibitory effect of AZD3241 was also observed in K562 and HepG cells that lack MPO enzymes. It suggested that endogenous CN as the primary substrate of SCN and SeCN could be generated by an MPO-like enzyme inhibited with AZD3241. Living mammalian cells contain some MPO-like enzymes that may also involve in mechanisms of endogenous CN production, which is needed to clarify in future sequencing experiments.

REFERENCE

- (1) Way, J. L. Cyanide Intoxication and Its Mechanism of Antagonism. *Annu. Rev. Pharmacol. Toxicol.* **1984**, 24 (1), 451–481. https://doi.org/10.1146/annurev.pa.24.040184.002315.
- (2) Gunasekar, P. G.; Sun, P. W.; Kanthasamy, A. G.; Borowitz, J. L.; Isom, G. E. Cyanide-Induced Neurotoxicity Involves Nitric Oxide and Reactive Oxygen Species Generation after N-Methyl-D-Aspartate Receptor Activation. *J. Pharmacol. Exp. Ther.* **1996**, 277 (1), 150–155.
- (3) Smolina, N.; Bruton, J.; Kostareva, A.; Sejersen, T. Assaying Mitochondrial Respiration as an Indicator of Cellular Metabolism and Fitness. *Methods Mol. Biol.* **2017**, *1601*, 79–87. https://doi.org/10.1007/978-1-4939-6960-9 7.
- (4) Hill, B. C.; Marmor, S. Photochemical and Ligand-Exchange Properties of the Cyanide Complex of Fully Reduced Cytochrome c Oxidase. *Biochem. J.* **1991**, *279* (*Pt 2* (Pt 2), 355–360. https://doi.org/10.1042/bj2790355.
- Van Buuren, K. J. H.; Nicholls, P.; Van Gelder, B. F. Biochemical and Biophysical Studies on Cytochrome Aa3. VI. Reaction of Cyanide with Oxidized and Reduced Enzyme. *Biochim. Biophys. Acta Bioenerg.* **1972**, *256* (2), 258–276. https://doi.org/https://doi.org/10.1016/0005-2728(72)90057-6.
- (6) Solomonson, L. P. Cyanide as a Metabolic Inhibitor; 1981.
- (7) YAMAMOTO, K.; YAMAMOTO, Y.; HATTORI, H.; SAMORI, T. Effects of Routes of Administration on the Cyanide Concentration Distribution in the Various Organs of Cyanide-Intoxicated Rats. *Tohoku J. Exp. Med.* **1982**, *137* (1), 73–78. https://doi.org/10.1620/tjem.137.73.
- (8) Saito, S. Influence of L-Cysteine and Hydroxocobalamin on Cyanide Distribution in Rats. 国立国会図書館デジタルコレクション **2001**.
- (9) Djerad, A.; Monier, C.; Houzé, P.; Borron, S. W.; Lefauconnier, J. M.; Baud, F. J. Effects of Respiratory Acidosis and Alkalosis on the Distribution of Cyanide into the Rat Brain. *Toxicol. Sci.* **2001**, *61* (2), 273–282. https://doi.org/10.1093/toxsci/61.2.273.
- (10) Ishii, A.; Seno, H.; Watanabe-Suzuki, K.; Suzuki, O.; Kumazawa, T. Determination of Cyanide in Whole Blood by Capillary Gas Chromatography with Cryogenic Oven Trapping. *Anal. Chem.* **1998**, *70* (22), 4873–4876. https://doi.org/10.1021/ac980498b.
- (11) Cipollone, R.; Visca, P. Is There Evidence That Cyanide Can Act as a Neuromodulator? *IUBMB Life* **2007**, *59* (3), 187–189. https://doi.org/10.1080/15216540600981768.
- (12) Weuffen, W.; Franzke, C.; Thurkow, B. [The Alimentary Ingestion, Analysis and Biological Significance of Thiocyanate]. *Nahrung* **1984**, *28* (4), 341–355. https://doi.org/10.1002/food.19840280403.
- (13) Makkar, H. P. S.; Siddhuraju, P.; Becker, K. Cyanogenic Glucosides/Cyanogens BT Plant Secondary Metabolites; Makkar, H. P. S., Siddhuraju, P., Becker, K., Eds.; Humana Press: Totowa, NJ, 2007; pp 61–65. https://doi.org/10.1007/978-1-59745-425-4 12.
- (14) Rao, P.; Singh, P.; Yadav, S. K.; Gujar, N. L.; Bhattacharya, R. Acute Toxicity of Some Synthetic Cyanogens in Rats: Time-Dependent Cyanide Generation and Cytochrome Oxidase Inhibition in Soft Tissues after Sub-Lethal Oral Intoxication. *Food Chem. Toxicol. an Int. J. Publ. Br. Ind. Biol. Res. Assoc.* **2013**, *59*, 595–609. https://doi.org/10.1016/j.fct.2013.06.035.
- (15) Shepherd, G.; Velez, L. I. Role of Hydroxocobalamin in Acute Cyanide Poisoning.

- Ann. Pharmacother. 2008, 42 (5), 661–669. https://doi.org/10.1345/aph.1K559.
- (16) Moir, D.; Rickert, W. S.; Levasseur, G.; Larose, Y.; Maertens, R.; White, P.; Desjardins, S. A Comparison of Mainstream and Sidestream Marijuana and Tobacco Cigarette Smoke Produced under Two Machine Smoking Conditions. *Chem. Res. Toxicol.* **2008**, *21* (2), 494–502. https://doi.org/10.1021/tx700275p.
- (17) Zgiczynski, J. M.; Stelmaszynska, T. Hydrogen Cyanide and Cyanogen Chloride Formation by the Myeloperoxidase-H2O2-Cl- System. *Biochim Biophys Acta* **1979**, 567 (2), 309–314. https://doi.org/10.1016/0005-2744(79)90116-5.
- (18) Ryall, B.; Davies, J. C.; Wilson, R.; Shoemark, A.; Williams, H. D. Pseudomonas Aeruginosa, Cyanide Accumulation and Lung Function in CF and Non-CF Bronchiectasis Patients. *Eur. Respir. J.* **2008**, *32* (3), 740 LP 747. https://doi.org/10.1183/09031936.00159607.
- (19) Broderick, K. E.; Chan, A.; Balasubramanian, M.; Feala, J.; Reed, S. L.; Panda, M.; Sharma, V. S.; Pilz, R. B.; Bigby, T. D.; Boss, G. R. Cyanide Produced by Human Isolates of Pseudomonas Aeruginosa Contributes to Lethality in Drosophila Melanogaster. *J. Infect. Dis.* **2008**, *197* (3), 457–464. https://doi.org/10.1086/525282.
- (20) Isom, G. E.; Borowitz, J. L.; Hall, A. H. Cyanide Metabolism and Physiological Disposition. In *Toxicology of Cyanides and Cyanogens*; 2016; pp 54–69. https://doi.org/10.1002/9781118628966.ch4.
- (21) McMahon, T. F.; Birnbaum, L. S. Age-Related Changes in Toxicity and Biotransformation of Potassium Cyanide in Male C57BL/6N Mice. *Toxicol Appl Pharmacol* **1990**, *105* (2), 305–314. https://doi.org/10.1016/0041-008x(90)90191-v.
- (22) Chaudhary, M.; Gupta, R. Cyanide Detoxifying Enzyme: Rhodanese. *Curr. Biotechnol. e* **2012**, *I* (4), 327–335. https://doi.org/10.2174/2211550111201040327.
- (23) Logue, B. A.; Hinkens, D. M.; Baskin, S. I.; Rockwood, G. A. The Analysis of Cyanide and Its Breakdown Products in Biological Samples. *Crit. Rev. Anal. Chem.* **2010**, *40* (2), 122–147. https://doi.org/10.1080/10408340903535315.
- (24) Auriga, M.; Koj, A. Protective Effect of Rhodanese on the Respiration of Isolated Mitochondria Intoxicated with Cyanide. *Bull. Acad. Pol. Sci. Biol.* **1975**, *23* (5), 305–310.
- (25) Nagahara, N.; Ito, T.; Kitamura, H.; Nishino, T. Tissue and Subcellular Distribution of Mercaptopyruvate Sulfurtransferase in the Rat: Confocal Laser Fluorescence and Immunoelectron Microscopic Studies Combined with Biochemical Analysis. *Histochem. Cell Biol.* **1998**, *110* (3), 243–250. https://doi.org/10.1007/s004180050286.
- (26) Campbell, R. E.; Kang, E. J.; Bastian, E.; Drake, M. A. The Use of Lactoperoxidase for the Bleaching of Fluid Whey. *J Dairy Sci* **2012**, *95* (6), 2882–2890. https://doi.org/10.3168/jds.2011-5166.
- (27) Fragoso, M. A.; Fernandez, V.; Forteza, R.; Randell, S. H.; Salathe, M.; Conner, G. E. Transcellular Thiocyanate Transport by Human Airway Epithelia. *J. Physiol.* **2004**, *561* (Pt 1), 183–194. https://doi.org/10.1113/jphysiol.2004.071548.
- (28) Toida, T.; Togawa, T.; Tanabe, S.; Imanari, T. Determination of Cyanide and Thiocyanate in Blood Plasma and Red Cells by High-Performance Liquid Chromatography with Fluorometric Detection. *J Chromatogr* **1984**, *308*, 133–141. https://doi.org/10.1016/s0021-9673(01)87540-3.
- (29) Vogel, S. N.; Sultan, T. R.; Ten Eyck, R. P. Cyanide Poisoning. *Clin Toxicol* **1981**, *18* (3), 367–383. https://doi.org/10.3109/15563658108990043.
- (30) Thomas, C.; Svehla, L.; Moffett, B. S. Sodium-Nitroprusside-Induced Cyanide Toxicity in Pediatric Patients. *Expert Opin Drug Saf* **2009**, *8* (5), 599–602. https://doi.org/10.1517/14740330903081717.

- (31) Schultz, C. P.; Ahmed, M. K.; Dawes, C.; Mantsch, H. H. Thiocyanate Levels in Human Saliva: Quantitation by Fourier Transform Infrared Spectroscopy. *Anal. Biochem.* **1996**, *240* (1), 7–12. https://doi.org/10.1006/abio.1996.0323.
- (32) Minarowski, Ł.; Sands, D.; Minarowska, A.; Karwowska, A.; Sulewska, A.; Gacko, M.; Chyczewska, E. Thiocyanate Concentration in Saliva of Cystic Fibrosis Patients. *Folia Histochem. Cytobiol.* **2008**, *46* (2), 245–246. https://doi.org/10.2478/v10042-008-0037-0.
- (33) Madiyal, A.; Ajila, V.; Babu, S. G.; Hegde, S.; Kumari, S.; Madi, M.; Achalli, S.; Alva, P.; Ullal, H. Status of Thiocyanate Levels in the Serum and Saliva of Non-Smokers, Ex-Smokers and Smokers. *Afr. Health Sci.* **2018**, *18* (3), 727–736. https://doi.org/10.4314/ahs.v18i3.31.
- (34) Leung, A. M.; Lamar, A.; He, X.; Braverman, L. E.; Pearce, E. N. Iodine Status and Thyroid Function of Boston-Area Vegetarians and Vegans. *J. Clin. Endocrinol. Metab.* **2011**, *96* (8), E1303-7. https://doi.org/10.1210/jc.2011-0256.
- (35) Lenney, W.; Gilchrist, F. J. Pseudomonas Aeruginosa and Cyanide Production. *Eur Respir J* **2011**, *37* (3), 482–483. https://doi.org/10.1183/09031936.00122810.
- (36) Sousa, A. B.; Manzano, H.; Soto-Blanco, B.; Górniak, S. L. Toxicokinetics of Cyanide in Rats, Pigs and Goats after Oral Dosing with Potassium Cyanide. *Arch. Toxicol.* **2003**, 77 (6), 330–334. https://doi.org/10.1007/s00204-003-0446-y.
- (37) Aminlari, M.; Vaseghi, T.; Kargar, M. A. The Cyanide-Metabolizing Enzyme Rhodanese in Different Parts of the Respiratory Systems of Sheep and Dog. *Toxicol. Appl. Pharmacol.* **1994**, *124* (1), 67–71. https://doi.org/10.1006/taap.1994.1009.
- (38) Salkowski, A. A.; Penney, D. G. Cyanide Poisoning in Animals and Humans: A Review. *Vet. Hum. Toxicol.* **1994**, *36* (5), 455–466.
- (39) Satu, M. S.; Lukey, B. J.; Romano, J. A.; Romano, J. A.; Salem, H. *Chemical Warfare Agents: Toxicity at Low Levels*; CRC Press, 2000.
- (40) Anan, Y.; Kimura, M.; Hayashi, M.; Koike, R.; Ogra, Y. Detoxification of Selenite to Form Selenocyanate in Mammalian Cells. *Chem Res Toxicol* **2015**, *28* (9), 1803–1814. https://doi.org/10.1021/acs.chemrestox.5b00254.
- (41) Bordo, D.; Bork, P. The Rhodanese/Cdc25 Phosphatase Superfamily. Sequence-Structure-Function Relations. *EMBO Rep.* **2002**, *3* (8), 741–746. https://doi.org/10.1093/embo-reports/kvf150.
- (42) Westley, J. Rhodanese. *Adv. Enzymol. Relat. Areas Mol. Biol.* **1973**, *39*, 327–368. https://doi.org/10.1002/9780470122846.ch5.
- (43) Mueller, E. G. Trafficking in Persulfides: Delivering Sulfur in Biosynthetic Pathways. *Nat. Chem. Biol.* **2006**, 2 (4), 185–194. https://doi.org/10.1038/nchembio779.
- (44) Vadhanavikit, S.; Kraus, R. J.; Ganther, H. E. Metabolism of Selenocyanate in the Rat. *Arch Biochem Biophys* **1987**, *258* (1), 1–6. https://doi.org/10.1016/0003-9861(87)90315-8.
- (45) Hartung, R. Cyanides and Nitriles. 3rd revise. John Wiley and Sons, Inc.: New York, NY pp 4845–4900.
- (46) Matthews, D. M.; Wilson, J.; Zilkha, K. J. Cyanide Metabolism and Vitamin B12 in Multiple Sclerosis. *J. Neurol. Neurosurg. Psychiatry* **1965**, *28* (5), 426–428. https://doi.org/10.1136/jnnp.28.5.426.
- (47) Ansell, M.; Lewis, F. A. A Review of Cyanide Concentrations Found in Human Organs. A Survey of Literature Concerning Cyanide Metabolism, "Normal", Non-Fatal, and Fatal Body Cyanide Levels. *J. Forensic Med.* **1970**, *17* (4), 148–155.
- (48) Lindsay, A. E.; Greenbaum, A. R.; O'Hare, D. Analytical Techniques for Cyanide in Blood and Published Blood Cyanide Concentrations from Healthy Subjects and

- Fire Victims. *Anal. Chim. Acta* **2004**, *511* (2), 185–195. https://doi.org/https://doi.org/10.1016/j.aca.2004.02.006.
- (49) Seto, Y. False Cyanide Detection. *Anal. Chem.* **2002**, *74* (5), 134A-141A. https://doi.org/10.1021/ac021967j.
- (50) Calafat, A. M.; Stanfill, S. B. Rapid Quantitation of Cyanide in Whole Blood by Automated Headspace Gas Chromatography. *J. Chromatogr. B, Anal. Technol. Biomed. life Sci.* **2002**, 772 (1), 131–137. https://doi.org/10.1016/s1570-0232(02)00067-3.
- (51) Xiaoyu, L.; Zihou, Y. High-Performance Liquid Chromatographic Determination of Thiocyanate Anion by Derivatization with Pentafluorobenzyl Bromide. *J. Chromatogr. A* **1993**, 653 (2), 348–353. https://doi.org/https://doi.org/10.1016/0021-9673(93)83194-W.
- (52) Lundquist, P.; Rosling, H.; Sörbo, B.; Tibbling, L. Cyanide Concentrations in Blood after Cigarette Smoking, as Determined by a Sensitive Fluorimetric Method. *Clin. Chem.* **1987**, *33* (7), 1228–1230.
- (53) Dirikolu, L.; Hughes, C.; Harkins, D.; Boyles, J.; Bosken, J.; Lehner, F.; Troppmann, A.; McDowell, K.; Tobin, T.; Sebastian, M. M.; Harrison, L.; Crutchfield, J.; Baskin, S. I.; Fitzgerald, T. D. The Toxicokinetics of Cyanide and Mandelonitrile in the Horse and Their Relevance to the Mare Reproductive Loss Syndrome. *Toxicol. Mech. Methods* 2003, 13 (3), 199–211. https://doi.org/10.1080/15376510309832.
- (54) Parmar, P.; Gupta, V. K.; Pillai, A. K. Rapid Spectrophotometric Determination of Trace Amounts of Cyanide and Hydrogen Cyanide Using P-Aminoacetanilide in Various Samples. *J. Korean Chem. Soc.* **2010**, *54* (1), 165–168.
- (55) Ganjeloo, A.; Isom, G. E.; Morgan, R. L.; Way, J. L. Fluorometric Determination of Cyanide in Biological Fluids with P-Benzoquinone. *Toxicol. Appl. Pharmacol.* **1980**, 55 (1), 103–107. https://doi.org/https://doi.org/10.1016/0041-008X(80)90225-2.
- (56) Pettigrew, A. R.; Fell, G. S. Simplified Colorimetric Determination of Thiocyanate in Biological Fluids, and Its Application to Investigation of the Toxic Amblyopias. *Clin. Chem.* **1972**, *18* (9), 996–1000.
- (57) McMillan, D. E.; Svoboda, A. C. 4th. The Role of Erythrocytes in Cyanide Detoxification. *J. Pharmacol. Exp. Ther.* **1982**, *221* (1), 37–42.
- (58) Dumas, P.; Gingras, G.; LeBlanc, A. Isotope Dilution-Mass Spectrometry Determination of Blood Cyanide by Headspace Gas Chromatography. *J. Anal. Toxicol.* **2005**, *29* (1), 71–75. https://doi.org/10.1093/jat/29.1.71.
- (59) Seto, Y.; Tsunoda, N.; Ohta, H.; Shinohara, T. Determination of Blood Cyanide by Headspace Gas Chromatography with Nitrogen-Phosphorus Detection and Using a Megabore Capillary Column. *Anal. Chim. Acta* **1993**, *276* (2), 247–259. https://doi.org/https://doi.org/10.1016/0003-2670(93)80391-W.
- (60) Felby, S. Determination of Cyanide in Blood by Reaction Head-Space Gas Chromatography. *Forensic Sci. Med. Pathol.* **2009**, 5 (1), 39–43. https://doi.org/10.1007/s12024-008-9069-1.
- (61) Gambaro, V.; Arnoldi, S.; Casagni, E.; Dell'acqua, L.; Pecoraro, C.; Froldi, R. Blood Cyanide Determination in Two Cases of Fatal Intoxication: Comparison between Headspace Gas Chromatography and a Spectrophotometric Method. *J. Forensic Sci.* **2007**, *52* (6), 1401–1404. https://doi.org/10.1111/j.1556-4029.2007.00570.x.
- (62) Zhang, C.; Zheng, H.; Ouyang, J.; Feng, S.; Taes, Y. E. C. Cyanide Distribution in Human Tissue, Determined by GC/ECD/HS. *Anal. Lett.* **2005**, *38* (2), 247–256. https://doi.org/10.1081/AL-200045143.
- (63) Dong, Y.-Y.; Li, C.-Y.; Zhang, X.-B.; Yu, R.-Q.; Shen, G.-L. A Novel Potentiometric Sensor for Thiocyanate Based on an Amide-Linked Manganese

- Diporphyrin Xanthene. *Electroanalysis* **2008**, *20* (16), 1769–1774. https://doi.org/https://doi.org/10.1002/elan.200804239.
- (64) Watanabe-Suzuki, K.; Ishii, A.; Suzuki, O. Cryogenic Oven-Trapping Gas Chromatography for Analysis of Volatile Organic Compounds in Body Fluids. *Anal. Bioanal. Chem.* **2002**, *373* (1–2), 75–80. https://doi.org/10.1007/s00216-002-1240-z.
- (65) Frison, G.; Zancanaro, F.; Favretto, D.; Ferrara, S. D. An Improved Method for Cyanide Determination in Blood Using Solid-Phase Microextraction and Gas Chromatography/Mass Spectrometry. *Rapid Commun. Mass Spectrom.* **2006**, *20* (19), 2932–2938. https://doi.org/10.1002/rcm.2689.
- (66) Murphy, K. E.; Schantz, M. M.; Butler, T. A.; Benner, B. A. J.; Wood, L. J.; Turk, G. C. Determination of Cyanide in Blood by Isotope-Dilution Gas Chromatography-Mass Spectrometry. *Clin. Chem.* **2006**, *52* (3), 458–467. https://doi.org/10.1373/clinchem.2005.061002.
- (67) Paul, B. D.; Smith, M. L. Cyanide and Thiocyanate in Human Saliva by Gas Chromatography-Mass Spectrometry. *J. Anal. Toxicol.* **2006**, *30* (8), 511–515. https://doi.org/10.1093/jat/30.8.511.
- (68) Kage, S.; Nagata, T.; Kudo, K. Determination of Cyanide and Thiocyanate in Blood by Gas Chromatography and Gas Chromatography-Mass Spectrometry. *J. Chromatogr. B. Biomed. Appl.* **1996**, 675 (1), 27–32. https://doi.org/10.1016/0378-4347(95)00344-4.
- Chen, S. H.; Wu, S. M.; Kou, H. S.; Wu, H. L. Electron-Capture Gas (69)Chromatographic Determination of Cyanide, Iodide, Nitrite, Sulfide, and Thiocyanate Anions by Phase-Transfer-Catalyzed Derivatization Bromide. Pentafluorobenzyl J. Anal.Toxicol. 1994, 18 81–85. (2),https://doi.org/10.1093/jat/18.2.81.
- (70) Sano, A.; Takezawa, M.; Takitani, S. High Performance Liquid Chromatography Determination of Cyanide in Urine by Pre-Column Fluorescence Derivatization. *Biomed. Chromatogr.* **1989**, *3* (5), 209–212. https://doi.org/10.1002/bmc.1130030507.
- (71) Sano, A.; Takimoto, N.; Takitani, S. High-Performance Liquid Chromatographic Determination of Cyanide in Human Red Blood Cells by Pre-Column Fluorescence Derivatization. *J. Chromatogr.* **1992**, *582* (1–2), 131–135. https://doi.org/10.1016/0378-4347(92)80311-d.
- (72) Mottier, N.; Jeanneret, F.; Rotach, M. Determination of Hydrogen Cyanide in Cigarette Mainstream Smoke by LC/MS/MS. *J. AOAC Int.* **2010**, *93* (3), 1032–1038. https://doi.org/10.1093/jaoac/93.3.1032.
- (73) Bhandari, R. K.; Manandhar, E.; Oda, R. P.; Rockwood, G. A.; Logue, B. A. Simultaneous High-Performance Liquid Chromatography-Tandem Mass Spectrometry (HPLC-MS-MS) Analysis of Cyanide and Thiocyanate from Swine Plasma. *Anal. Bioanal. Chem.* **2014**, *406* (3), 727–734. https://doi.org/10.1007/s00216-013-7536-3.
- (74) Mochizuki, R.; Higashi, K.; Okamoto, Y.; Abe, H.; Iwase, H.; Toida, T. Detection of Selenocyanate in Biological Samples by HPLC with Fluorescence Detection Using Konig Reaction. *Chem Pharm Bull* **2019**, *67* (8), 884–887. https://doi.org/10.1248/cpb.c19-00277.
- (75) Chinaka, S.; Takayama, N.; Michigami, Y.; Ueda, K. Simultaneous Determination of Cyanide and Thiocyanate in Blood by Ion Chromatography with Fluorescence and Ultraviolet Detection. *J. Chromatogr. B Biomed. Sci. Appl.* **1998**, 713 (2), 353–359. https://doi.org/https://doi.org/10.1016/S0378-4347(98)00176-5.

- (76) Logue, B. A.; Kirschten, N. P.; Petrikovics, I.; Moser, M. A.; Rockwood, G. A.; Baskin, S. I. Determination of the Cyanide Metabolite 2-Aminothiazoline-4-Carboxylic Acid in Urine and Plasma by Gas Chromatography-Mass Spectrometry. *J. Chromatogr. B, Anal. Technol. Biomed. life Sci.* **2005**, *819* (2), 237–244. https://doi.org/10.1016/j.jchromb.2005.01.045.
- (77) Youso, S. L.; Rockwood, G. A.; Lee, J. P.; Logue, B. A. Determination of Cyanide Exposure by Gas Chromatography-Mass Spectrometry Analysis of Cyanide-Exposed Plasma Proteins. *Anal. Chim. Acta* **2010**, *677* (1), 24–28. https://doi.org/10.1016/j.aca.2010.01.028.
- (78) Introduction to Fluorescence BT Principles of Fluorescence Spectroscopy; Lakowicz, J. R., Ed.; Springer US: Boston, MA, 2006; pp 1–26. https://doi.org/10.1007/978-0-387-46312-4 1.
- (79) Rodkey, F. L.; Collison, H. A. Determination of Cyanide and Nitroprusside in Blood and Plasma. *Clin. Chem.* **1977**, *23* (11), 1969–1975.
- (80) Nagashima, S. Simultaneous Reaction Rate Spectrophotometric Determination of Cyanide and Thiocyanate by Use of the Pyridine-Barbituric Acid Method. *Anal. Chem.* **1984**, *56* (11), 1944–1947. https://doi.org/10.1021/ac00275a042.
- (81) Bulska, E.; Wagner, B. Quantitative Aspects of Inductively Coupled Plasma Mass Spectrometry. *Philos. Trans. A. Math. Phys. Eng. Sci.* **2016**, *374*. https://doi.org/10.1098/rsta.2015.0369.
- (82) Wilschefski, S. C.; Baxter, M. R. Inductively Coupled Plasma Mass Spectrometry: Introduction to Analytical Aspects. *Clin. Biochem. Rev.* **2019**, *40* (3), 115–133. https://doi.org/10.33176/AACB-19-00024.
- (83) Rausch, P. G.; Moore, T. G. Granule Enzymes of Polymorphonuclear Neutrophils: A Phylogenetic Comparison. *Blood* **1975**, *46* (6), 913–919.
- (84) Klebanoff, S. J.; Rosen, H. The Role of Myeloperoxidase in the Microbicidal Activity of Polymorphonuclear Leukocytes. *Ciba Found. Symp.* **1978**, No. 65, 263–284. https://doi.org/10.1002/9780470715413.ch15.
- (85) Arnhold, J.; Flemmig, J. Human Myeloperoxidase in Innate and Acquired Immunity. *Arch. Biochem. Biophys.* **2010**, 500 (1), 92–106. https://doi.org/10.1016/j.abb.2010.04.008.
- (86) Rosen, H.; Crowley, J. R.; Heinecke, J. W. Human Neutrophils Use the Myeloperoxidase-Hydrogen Peroxide-Chloride System to Chlorinate but Not Nitrate Bacterial Proteins during Phagocytosis. *J. Biol. Chem.* **2002**, *277* (34), 30463–30468. https://doi.org/10.1074/jbc.M202331200.
- (87) San Gabriel, P. T.; Liu, Y.; Schroder, A. L.; Zoellner, H.; Chami, B. The Role of Thiocyanate in Modulating Myeloperoxidase Activity during Disease. *International Journal of Molecular Sciences*. 2020. https://doi.org/10.3390/ijms21176450.
- (88) Chami, B.; Martin, N. J. J.; Dennis, J. M.; Witting, P. K. Myeloperoxidase in the Inflamed Colon: A Novel Target for Treating Inflammatory Bowel Disease. *Arch. Biochem. Biophys.* **2018**, *645*, 61–71. https://doi.org/10.1016/j.abb.2018.03.012.
- (89) Ndrepepa, G. Myeloperoxidase A Bridge Linking Inflammation and Oxidative Stress with Cardiovascular Disease. *Clin. Chim. Acta.* **2019**, *493*, 36–51. https://doi.org/10.1016/j.cca.2019.02.022.
- (90) Yamalik, N.; Cağlayan, F.; Kilinç, K.; Kilinç, A.; Tümer, C. The Importance of Data Presentation Regarding Gingival Crevicular Fluid Myeloperoxidase and Elastase-like Activity in Periodontal Disease and Health Status. *J. Periodontol.* **2000**, *71* (3), 460–467. https://doi.org/10.1902/jop.2000.71.3.460.
- (91) Tzikas, S.; Schlak, D.; Sopova, K.; Gatsiou, A.; Stakos, D.; Stamatelopoulos, K.; Stellos, K.; Laske, C. Increased Myeloperoxidase Plasma Levels in Patients with

- Alzheimer's Disease. *J. Alzheimers. Dis.* **2014**, *39* (3), 557–564. https://doi.org/10.3233/JAD-131469.
- (92) Gunasekar, P. G.; Borowitz, J. L.; Turek, J. J.; Van Horn, D. A.; Isom, G. E. Endogenous Generation of Cyanide in Neuronal Tissue: Involvement of a Peroxidase System. *J Neurosci Res* **2000**, *61* (5), 570–575. https://doi.org/10.1002/1097-4547(20000901)61:5<570::AID-JNR12>3.0.CO;2-V.
- (93) Galijasevic, S. The Development of Myeloperoxidase Inhibitors. *Bioorg. Med. Chem. Lett.* **2019**, 29 (1), 1–7. https://doi.org/https://doi.org/10.1016/j.bmcl.2018.11.031.
- (94) Jacob 3rd, P.; Savanapridi, C.; Yu, L.; Wilson, M.; Shulgin, A. T.; Benowitz, N. L.; Elias-Baker, B. A.; Hall, S. M.; Herning, R. I.; Jones, R. T.; et al. Ion-Pair Extraction of Thiocyanate from Plasma and Its Gas Chromatographic Determination Using on-Column Alkylation. *Anal Chem* **1984**, *56* (9), 1692–1695. https://doi.org/10.1021/ac00273a036.
- (95) Toida, T.; Tanabe, S.; Imanari, T. Fluorometric Determination of Cyanide and Thiocyanate by Koenig Reaction. *Chem. Pharm. Bull. (Tokyo).* **1981**, *29* (12), 3763–3764. https://doi.org/10.1248/cpb.29.3763.
- (96) Luo, P.; Yu, Y.; Wu, D.; Li, X.; Dai, C.; Chen, X.; Li, G.; Wu, Y. Simultaneous Determination of Cyanide and Thiocyanate in Swine Plasma by High-Performance Liquid Chromatography with Fluorescence Detection Based on a Novel D–π–A Carbazole-Based Turn-on Fluorescence Labeling Reagent. *Anal. Methods* 2019, 11 (23), 2983–2990. https://doi.org/10.1039/c9ay00784a.
- (97) Lundquist, P.; Kagedal, B.; Nilsson, L. An Improved Method for Determination of Thiocyanate in Plasma and Urine. *Eur J Clin Chem Clin Biochem* **1995**, *33* (6), 343–349. https://doi.org/10.1515/cclm.1995.33.6.343.
- (98) Shin, Y. G.; Meijering, H.; Heuveln, F. van; Wieling, J.; Halladay, J. S.; Sahasranaman, S.; Hop, C. E. Validation of a Method for the Determination of Thiocyanate in Human Plasma by UV/VIS Spectrophotometry and Application to a Phase I Clinical Trial of GDC-0425; 2015.
- (99) Saussereau, E.; Goulle, J. P.; Lacroix, C. Determination of Thiocyanate in Plasma by Ion Chromatography and Ultraviolet Detection. *J Anal Toxicol* **2007**, *31* (7), 383–387. https://doi.org/10.1093/jat/31.7.383.
- (100) Tsuge, K.; Kataoka, M.; Seto, Y. Cyanide and Thiocyanate Levels in Blood and Saliva of Healthy Adult Volunteers. *J. Heal. Sci.* **2000**, *46* (5), 343–350. https://doi.org/10.1248/jhs.46.343.
- (101) Chandler, J. D.; Horati, H.; Walker, D. I.; Pagliano, E.; Tirouvanziam, R.; Veltman, M.; Scholte, B. J.; Janssens, H. M.; Go, Y. M.; Jones, D. P. Determination of Thiocyanate in Exhaled Breath Condensate. *Free Radic Biol Med* **2018**, *126*, 334–340. https://doi.org/10.1016/j.freeradbiomed.2018.08.012.
- (102) Zhang, L.; Fang, C.; Liu, L.; Liu, X.; Fan, S.; Li, J.; Zhao, Y.; Ni, S.; Liu, S.; Wu, Y. A Case-Control Study of Urinary Levels of Iodine, Perchlorate and Thiocyanate and Risk of Papillary Thyroid Cancer. *Environ. Int.* **2018**, *120*, 388–393. https://doi.org/10.1016/j.envint.2018.08.024.
- (103) Holzbecher, M.; Ellenberger, H. A. An Evaluation and Modification of a Microdiffusion Method for the Emergency Determination of Blood Cyanide. *J. Anal. Toxicol.* **1985**, *9* (6), 251–253. https://doi.org/10.1093/jat/9.6.251.
- (104) Felscher, D.; Wulfmeyer, M. A New Specific Method to Detect Cyanide in Body Fluids, Especially Whole Blood, by Fluorimetry. *J. Anal. Toxicol.* **1998**, *22* (5), 363–366. https://doi.org/10.1093/jat/22.5.363.
- (105) Imanari, T.; Tanabe, S.; Toida, T. Simultaneous Determination of Cyanide and

- Thiocyanate by High Performance Liquid Chromatography. *Chem Pharm Bull* **1982**, 30 (10), 3800–3802. https://doi.org/10.1248/cpb.30.3800.
- (106) Soleimani, M.; Yamini, Y.; Mohazab Rad, F. A Simple and High Resolution Ion-Pair HPLC Method for Separation and Simultaneous Determination of Nitrate and Thiocyanate in Different Water Samples. *J Chromatogr Sci* **2012**, *50* (9), 826–830. https://doi.org/10.1093/chromsci/bms078.
- (107) Pagliano, E.; LeBlanc, K. L.; Mester, Z. Selective Gas Chromatography Mass Spectrometry Method for Ultratrace Detection of Selenocyanate. *Anal Chem* **2019**, *91* (19), 12162–12166. https://doi.org/10.1021/acs.analchem.9b02615.
- (108) LeBlanc, K. L.; Smith, M. S.; Wallschlager, D. Production and Release of Selenocyanate by Different Green Freshwater Algae in Environmental and Laboratory Samples. *Env. Sci Technol* **2012**, *46* (11), 5867–5875. https://doi.org/10.1021/es203904e.
- (109) Burgess, V. A.; Easton, C. J.; Hay, M. P. Selective Reaction of Glycine Residues in Hydrogen Atom Transfer from Amino Acid Derivatives. *J. Am. Chem. Soc.* **1989**, *111* (3), 1047–1052. https://doi.org/10.1021/ja00185a039.
- (110) Mateus, F. H.; Lepera, J. S.; Lanchote, V. L. Determination of Acetonitrile and Cyanide in Rat Blood: Application to an Experimental Study. *J. Anal. Toxicol.* **2005**, 29 (2), 105–109. https://doi.org/10.1093/jat/29.2.105.
- (111) KANAI, R.; HASHIMOTO, K. DETERMINATION OF ACRYLONITRILE, CYANIDE AND THIOCYANATE IN BIOLOGICAL MATERIALS. *Ind. Health* **1965**, *3* (1–2), 47–52. https://doi.org/10.2486/indhealth.3.47.
- (112) Lin, X.; Hasi, W.-L.-J.; Lou, X.-T.; Lin, S.; Yang, F.; Jia, B.-S.; Cui, Y.; Ba, D.-X.; Lin, D.-Y.; Lu, Z.-W. Rapid and Simple Detection of Sodium Thiocyanate in Milk Using Surface-Enhanced Raman Spectroscopy Based on Silver Aggregates. *J. Raman Spectrosc.* **2014**, 45 (2), 162–167. https://doi.org/https://doi.org/10.1002/jrs.4436.
- (113) Simpson, D. M.; Beynon, R. J. Acetone Precipitation of Proteins and the Modification of Peptides. *J. Proteome Res.* **2010**, *9* (1), 444–450. https://doi.org/10.1021/pr900806x.
- (114) Polson, C.; Sarkar, P.; Incledon, B.; Raguvaran, V.; Grant, R. Optimization of Protein Precipitation Based upon Effectiveness of Protein Removal and Ionization Effect in Liquid Chromatography-Tandem Mass Spectrometry. *J. Chromatogr. B, Anal. Technol. Biomed. life Sci.* **2003**, 785 (2), 263–275. https://doi.org/10.1016/s1570-0232(02)00914-5.
- (115) Rezacova, K.; Canova, K.; Bezrouk, A.; Rudolf, E. Selenite Induces DNA Damage and Specific Mitochondrial Degeneration in Human Bladder Cancer Cells. *Toxicol Vitr.* **2016**, *32*, 105–114. https://doi.org/10.1016/j.tiv.2015.12.011.
- (116) Kim, E. H.; Sohn, S.; Kwon, H. J.; Kim, S. U.; Kim, M. J.; Lee, S. J.; Choi, K. S. Sodium Selenite Induces Superoxide-Mediated Mitochondrial Damage and Subsequent Autophagic Cell Death in Malignant Glioma Cells. *Cancer Res* **2007**, 67 (13), 6314–6324. https://doi.org/10.1158/0008-5472.CAN-06-4217.
- (117) Kim, E. H.; Choi, K. S. A Critical Role of Superoxide Anion in Selenite-Induced Mitophagic Cell Death. *Autophagy* **2008**, *4* (1), 76–78. https://doi.org/10.4161/auto.5119.
- (118) Zhao, R.; Xiang, N.; Domann, F. E.; Zhong, W. Expression of P53 Enhances Selenite-Induced Superoxide Production and Apoptosis in Human Prostate Cancer Cells. *Cancer Res* **2006**, *66* (4), 2296–2304. https://doi.org/10.1158/0008-5472.CAN-05-2216.
- (119) Park, S. H.; Kim, J. H.; Chi, G. Y.; Kim, G. Y.; Chang, Y. C.; Moon, S. K.; Nam, S.

- W.; Kim, W. J.; Yoo, Y. H.; Choi, Y. H. Induction of Apoptosis and Autophagy by Sodium Selenite in A549 Human Lung Carcinoma Cells through Generation of Reactive Oxygen Species. *Toxicol Lett* **2012**, *212* (3), 252–261. https://doi.org/10.1016/j.toxlet.2012.06.007.
- (120) Seko, Y.; Imura, N. Active Oxygen Generation as a Possible Mechanism of Selenium Toxicity. *Biomed Env. Sci* **1997**, *10* (2–3), 333–339.
- (121) Chaudiere, J.; Courtin, O.; Leclaire, J. Glutathione Oxidase Activity of Selenocystamine: A Mechanistic Study. *Arch Biochem Biophys* **1992**, *296* (1), 328–336. https://doi.org/10.1016/0003-9861(92)90580-p.
- (122) Spallholz, J. E. On the Nature of Selenium Toxicity and Carcinostatic Activity. *Free Radic Biol Med* **1994**, *17* (1), 45–64. https://doi.org/10.1016/0891-5849(94)90007-8.
- (123) Ngogang, J.; Eben-Moussi, E.; Raisonnier, A. [Salivary, urinary and plasma thiocyanate in smokers and non-smokers]. *Pathol Biol* **1983**, *31* (3), 155–160.
- (124) Borowitz, J. L.; Rathinavelu, A.; Kanthasamy, A.; Wilsbacher, J.; Isom, G. E. Accumulation of Labeled Cyanide in Neuronal Tissue. *Toxicol Appl Pharmacol* **1994**, *129* (1), 80–85. https://doi.org/10.1006/taap.1994.1230.
- (125) Gunasekar, P. G.; Borowitz, J. L.; Turek, J. J.; Van Horn, D. A.; Isom, G. E. Endogenous Generation of Cyanide in Neuronal Tissue: Involvement of a Peroxidase System. *J Neurosci Res* **2000**, *61* (5), 570–575. https://doi.org/10.1002/1097-4547(20000901)61:5<570::AID-JNR12>3.0.CO;2-V.
- (126) Ahmad, G.; Chami, B.; Liu, Y.; Schroder, A. L.; San Gabriel, P. T.; Gao, A.; Fong, G.; Wang, X.; Witting, P. K. The Synthetic Myeloperoxidase Inhibitor AZD3241 Ameliorates Dextran Sodium Sulfate Stimulated Experimental Colitis. *Front. Pharmacol.* **2020**, *11*, 556020. https://doi.org/10.3389/fphar.2020.556020.
- (127) Chung, J.; Wood, J. L. Oxidation of Thiocyanate to Cyanide and Sulfate by the Lactoperoxidase-Hydrogen Peroxide System. *Arch. Biochem. Biophys.* **1970**, *141* (1), 73–78. https://doi.org/https://doi.org/10.1016/0003-9861(70)90108-6.
- (128) Morris, D. R.; Hager, L. P. Chloroperoxidase: I. ISOLATION AND PROPERTIES OF THE CRYSTALLINE GLYCOPROTEIN. *J. Biol. Chem.* **1966**, *241* (8), 1763–1768. https://doi.org/10.1016/S0021-9258(18)96701-3.
- (129) Chung, J.; Wood, J. L. Oxidation of Thiocyanate to Cyanide Catalyzed by Hemoglobin. *J. Biol. Chem.* **1971**, 246 (3), 555–560. https://doi.org/https://doi.org/10.1016/S0021-9258(18)62450-0.

Publication

This work was published as the following article.

Aphinan Hongprasit, Yusuke Okamoto, Toshihiko Toida, Yasumitsu Ogra: Comparison of quantification of selenocyanate and thiocyanate in cultured mammalian cells between HPLC-fluorescence detector and HPLC-inductively coupled plasma mass spectrometer. J Chromatogr B Analyt Technol Biomed Life Sci. 2021, 1181, 122924.

doi: 10.1016/j.jchromb.2021.122924. Epub 2021 Sep 4.

Reveiwers

This work, for the doctoral degree of Pharmacetucal Sciences, was examined by the following reviewers authorized by Graduate School of Pharmaceutical Sciences, Chiba University, Japan.

Chief Reviewer: Professor Kosei Itoh (Chiba University)

Reviewer: Professor Motoyuki Itoh (Chiba University)

Reviewer: Professor Daisuke Nakajima (National Institute of Environmental

Studies, Japan)